Physica D 241 (2012) 1026–1042

Contents lists available at SciVerse ScienceDirect

Physica D

journal homepage: www.elsevier.com/locate/physd

Influence of planetary oblateness on Keplerian dynamics in magnetospheres and existence of invariant tori

Manuel Iñarrea [a], Víctor Lanchares [b], Jesús F. Palacián [c,*], Ana I. Pascual [b], J. Pablo Salas [a], Patricia Yanguas [c]

[a] Universidad de La Rioja, Área de Física Aplicada, 26006 Logroño, Spain
[b] Universidad de La Rioja, Departamento de Matemáticas y Computación, 26004 Logroño, Spain
[c] Universidad Pública de Navarra, Departamento de Ingeniería Matemática e Informática, 31006 Pamplona, Spain

ARTICLE INFO

Article history:
Received 15 November 2010
Received in revised form
26 December 2011
Accepted 24 February 2012
Available online 3 March 2012
Communicated by A. Doelman

Keywords:
Störmer problem
Perturbed Kepler problems
Symmetries and reduction
Relative equilibria
Quasiperiodic solutions
Invariant tori

ABSTRACT

The problem of the dynamics of a charged particle orbiting around a rotating magnetic planet is revisited, the goal being twofold. On the one hand the model takes into account, apart from the magnetic and the electric field, the gravitational potential of the planet where the effect of the planetary oblateness is also incorporated. The techniques used in this analysis include averaging with respect to the mean anomaly, reduction to the simplest possible reduced space, study of the possible relative equilibria with the occurring parametric bifurcations and the stability analysis of these equilibria using normal forms. Also, we prove the existence of KAM 3-tori of the original system from the relative equilibria that are elliptic points in the fully-reduced space.

1. Introduction

For many years, physicists and astronomers have paid much attention to the study of the motion of charged dust in planetary magnetospheres. Today, it is still an issue of interest, mainly from the point of view of planetary mission design [1]. Needless to say, many of the studies of recent years have been motivated by the Cassini mission, which performed detailed in situ measurements of charged dust grains orbiting around Saturn.

From the theoretical point of view, since the pioneering works of Störmer (see the papers [2] and the monograph [3]), where the motion of a light charge in a pure magnetic dipole field (the Störmer model) is considered, to more complex models for heavier particles where the gravity is also considered (see [4,5] and references therein), this interest has resulted in a plethora of papers where different models and approaches have been used in order to describe the single-particle dynamics of charged dust orbiting magnetic planets. In particular, Horányi, Howard and coworkers [6–8], using a model that includes Keplerian gravity, a magnetic dipole aligned along the axis of rotation of the planet and a corotational electric field, showed that the dynamics of the charged dust grain is governed by a two-dimensional effective potential. From this potential the above-mentioned authors obtain the global stability conditions of the grain [7] and they predict the existence of non-equatorial halo orbits [8,9] for the grain.

The model proposed by the aforementioned authors is a nice candidate to which to apply the modern analytic tools of nonlinear dynamics. Then, in [4,10] we performed on that model a perturbative analytical study of the Keplerian regime of the problem. Among other things, we studied the flow of the resulting (averaged) system in the most reduced phase space, describing the existing relative equilibria, their stability and bifurcations. Finally, we connected the analysis of the flow on these reduced phase spaces with that of the original system.

In the present work we go one step further by considering the influence of the planetary oblateness. Our aim is to perform a qualitative analysis of the three-degree-of-freedom Hamiltonian system. The dynamics depends on three external parameters: δ (the ratio between the magnetic and the Keplerian interactions), β (the ratio between the electrostatic and Keplerian interactions) and J_2 (the planet's oblateness) and on one internal parameter: the third component of the angular momentum vector. We will analyse the influence in the dynamics of the introduction in the model of the planet's oblateness and we will compare the results with those obtained in [4]. This is the first main contribution of the paper.

* Corresponding author. Tel.: +34 948 169554; fax: +34 948 169521.
E-mail address: palacian@unavarra.es (J.F. Palacián).

0167-2789/$ – see front matter © 2012 Elsevier B.V. All rights reserved.
doi:10.1016/j.physd.2012.02.017

The scheme of our procedure is as follows. We normalise (average) the Hamiltonian with respect to the mean anomaly of the motion of the particle, and reduce the Hamiltonian function by the symmetry related to the (approximate) integral introduced by the averaging. We reduce again by the (exact) axial symmetry of the problem, which allows us to pass to a new Hamiltonian function defining a dynamical system of one degree of freedom. The discrete symmetries of the original Hamiltonian allows us to further reduce the Hamiltonian, introducing the appropriate invariants that defined the fully-reduced space, without decreasing the number of degrees of freedom of the system. Once the system is completely reduced, we analyse the relative equilibria, their linear and nonlinear stability and the bifurcations of the fully-reduced equations using techniques based on the discussion of roots of polynomials and appropriate normal forms around equilibria. The final step entails extracting the corresponding consequences on the flow of the original Hamiltonian using reconstruction techniques, which is our second main contribution.

The paper is organised into seven sections. The model Hamiltonian of the problem is presented in Section 2. As we restrict our model to the Keplerian regime, a normalisation of Delaunay of the equations of motion is made in Section 3. In Section 4 we perform the reductions related to the symmetries of the problem. We start with the Keplerian reduction originated after normalising over the mean anomaly and truncating the higher-order terms. Without decreasing the number of degrees of freedom of the system, the discrete symmetries of the original Hamiltonian allow us to further reduce the averaged Hamiltonian to a fully-reduced phase space. Section 5 is devoted to the analysis of the fully-reduced Hamiltonian, discussing the relative equilibria, their stability and the occurring bifurcations. In Section 6 the flow corresponding with the Hamiltonian that defines a system of three degrees of freedom is reconstructed from the analysis carried out in the reduced space. We end up with the existence of invariant 2-tori that bifurcate according to the bifurcation lines (a bit distorted) discussed in Section 5. We also show the existence of KAM 3-tori. The conclusions are drawn in Section 7.

2. The problem

We consider a particle of mass m and electric charge q orbiting around a non-spherical rotating magnetic planet of mass M and equatorial radius R_p. The general Hamiltonian of this particle in Gaussian units can be expressed as

$$\mathcal{H} = \frac{1}{2\,m}\left(\mathbf{P} - \frac{q}{c}\,\mathbf{A}\right)^2 + U(\mathbf{x}), \tag{1}$$

where c is the speed of light, $\mathbf{x} = (x, y, z)$ is the particle position in Cartesian coordinates and $\mathbf{P} = (P_x, P_y, P_z)$ are their conjugate momenta. The vector potential $\mathbf{A}$ describes the magnetic forces and the scalar potential $U(\mathbf{x})$ accounts for the electrostatic and gravitational interactions. We consider that the magnetic field $\mathbf{B}$ is created by a perfect magnetic dipole of strength μ aligned along the north–south poles of the planet (the z-axis). Therefore, the vectors $\mathbf{A}$ and $\mathbf{B}$ are given by

$$\mathbf{A} = \frac{\mu}{r^3}(-y, x, 0), \qquad \mathbf{B} = \nabla \times \mathbf{A}, \tag{2}$$

where $r = (x^2 + y^2 + z^2)^{1/2}$ is the distance of the charged particle to the centre of mass of the planet.

By assuming that the magnetosphere surrounding the planet is a rigid conducting plasma which rotates with the same angular velocity ω as the planet, the charged particle is subject to a corotational static electric field $\mathbf{E}$ of the form

$$\mathbf{E} = -\frac{1}{c}\,(\mathbf{\Omega} \times \mathbf{x}) \times \mathbf{B} = -\frac{\mu\,\omega}{c}\,\nabla\,\Psi$$
$$\text{where } \Psi = \frac{x^2 + y^2}{r^3},\ \ \mathbf{\Omega} = (0, 0, \omega).$$

Due to the non-sphericity of the planet, besides the pure Keplerian term $U_K = -M\,m/r$, the gravitational potential of our model includes the so called J_2 term [11]

$$U_{J_2} = \frac{M\,m\,R_p^2 J_2}{2\,r^3}\left(\frac{3\,z^2}{r^2} - 1\right).$$

The dimensionless parameter J_2 accounts for the non-sphericity of the planet. This parameter is positive for an oblate planet, and negative for a prolate one.

Therefore, the combined action of the gravitational and electrostatic interactions is given by the scalar potential $U(\mathbf{x})$

$$\begin{aligned} U(\mathbf{x}) &= U_K + U_{J_2} + U_e \\ &= -\frac{M\,m}{r} + \frac{M\,m\,R_p^2 J_2}{2\,r^3}\left(\frac{3\,z^2}{r^2} - 1\right) + \frac{q\,\mu\,\omega}{c}\Psi, \end{aligned} \tag{3}$$

where $U_e = q\,\mu\,\omega\,\Psi/c$ is the electrostatic potential. By introducing the expressions (2) and (3) into (1) the resulting Hamiltonian yields

$$\begin{aligned} \mathcal{H} &= \frac{1}{2\,m}\left(P_x^2 + P_y^2 + P_z^2\right) - \frac{M\,m}{r} + \frac{M\,m\,R_p^2 J_2}{2\,r^3}\left(\frac{3\,z^2}{r^2} - 1\right) \\ &\quad + \frac{q\,\mu\,\omega}{c}\,\Psi + \frac{\mu\,q}{m\,c\,r^3}\left(\frac{\mu\,q}{2\,c}\,\frac{x^2 + y^2}{r^3} - P_\phi\right), \end{aligned}$$

where $P_\phi = x\,P_y - y\,P_x$ is the z-component of the angular momentum.

Since the above Hamiltonian $\mathcal{H}$ is invariant under rotations around the z-axis, cylindrical variables $(\rho, z, \phi, P_\rho, P_z, P_\phi)$ arise in a natural way and in these coordinates the Hamiltonian reads as

$$\begin{aligned} \mathcal{H} &= \frac{1}{2\,m}\left(P_\rho^2 + P_z^2 + \frac{P_\phi^2}{\rho^2}\right) - \frac{M\,m}{r} + \frac{M\,m\,R_p^2 J_2}{2\,r^3}\left(\frac{3\,z^2}{r^2} - 1\right) \\ &\quad + \frac{m\,\omega\,\omega_c\,R_p^3}{c}\,\frac{\rho^2}{r^3} + \frac{\omega_c\,R_p^3}{r^3}\left(\frac{m\,\omega_c\,R_p^3}{2}\,\frac{\rho^2}{r^3} - P_\phi\right). \end{aligned}$$

The parameter $\omega_c = (q\,B_o)/(m\,c)$ is the cyclotron frequency, where $B_o = \mu/(R_p^3\,c)$ designates the magnetic field strength at the planetary equator.

If we scale positions as $\mathbf{x}' = \mathbf{x}/R_p$ and time as $t' = \omega_K\,t$, where $\omega_K = (M/R_p^3)^{1/2}$ is the Keplerian frequency, we arrive at the dimensionless Hamiltonian

$$\begin{aligned} \mathcal{H}' &= \frac{\mathcal{H}}{m\,R_p^2\,\omega_K^2} \\ &= \frac{1}{2}\left(P_\rho^2 + P_z^2 + \frac{P_\phi^2}{\rho^2}\right) + U_K + U_{J_2} + U_e + U_m \\ &= \frac{1}{2}\left(P_\rho^2 + P_z^2 + \frac{P_\phi^2}{\rho^2}\right) - \frac{1}{r} + \frac{J_2}{2\,r^3}\left(\frac{3\,z^2}{r^2} - 1\right) \\ &\quad + \delta\,\beta\,\frac{\rho^2}{r^3} + \frac{\delta}{r^3}\left(\frac{\delta\,\rho^2}{2\,r^3} - P_\phi\right). \end{aligned} \tag{4}$$

In the previous Hamiltonian we have dropped the primes and two new parameters have been defined: $\delta = \omega_c/\omega_K$ and $\beta = \omega/\omega_K > 0$. The parameter δ indicates the ratio between the magnetic and the Keplerian interactions (i.e. the charge–mass ratio q/m of the particle), and β refers to the ratio between the electrostatic and Keplerian interactions.

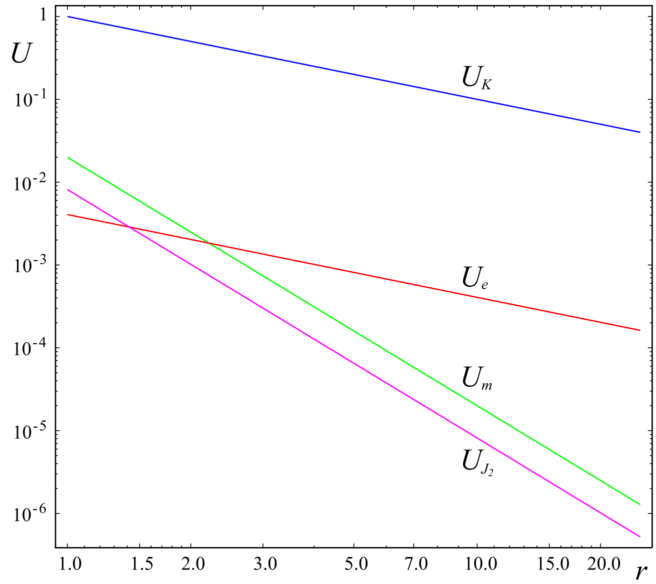

Fig. 1. Variation of the potentials U_K, U_e, U_m, U_{J_2} in the equatorial plane ($z = 0$) as a function of the distance r for the case of Saturn and a charged particle with $\delta = 0.01$ and $P_\phi = 2$.

For a given planet, the parameters β and J_2 take constant values, hence the problem depends on three parameters. On the one hand, it depends on two internal parameters: P_ϕ and the energy $E = \mathcal{H}'$. On the other hand, the problem depends on the external parameter δ, which can be positive or negative depending on the charge of the particle.

The goal of this paper is to study the dynamics of the system when the main effect on the particle is assumed to be the pure Keplerian gravity. Therefore, we assume that the Keplerian potential U_K is only slightly affected by the other potential terms, U_e, U_m, U_{J_2}. That is, $U_K \gg U_e, U_m, U_{J_2}$.

For example, in the case of Saturn, the most oblate planet of the Solar System, the values of the constant parameters are $\beta = 0.40649$ and $J_2 = 0.016298$, see [11,12]. In order to keep the potentials U_e and U_m as perturbations of the Keplerian potential U_K, we shall specify that the external parameter δ varies in $[-0.01, 0.01]$. For more details on the ranges of validity of δ, see [13]. We will use these numerical values in some computations.

Fig. 1 shows the variation on a double logarithmic scale of the potentials U_K, U_e, U_m, U_{J_2} as a function of the distance r for the case of Saturn in the equatorial plane ($z = 0$) for a charged particle with $\delta = 0.01$ and $P_\phi = 2$. From this figure it is clear that, for those parameter values, the main interaction is the pure Keplerian gravitational potential, so that the remaining potential terms can be regarded as perturbations because they are several orders of magnitude lower. It is also clear that for this planet it is important to include in the study the U_{J_2} term in the gravitational potential because it is of similar magnitude to the electromagnetic perturbations. A similar comparison about the influence of the forces acting on the particles appears in [14].

From now on we will take the small parameter to be of the size of δ while J_2 will be supposed to be another small parameter of the same order as δ.

3. Delaunay normalisation through first-order averaging

We start by introducing two sets of coordinates that are suitable for working with Keplerian systems. The first set is given by the polar-nodal coordinates $(r, \vartheta, h, R, G, H)$, where r stands for the radial distance from the centre of the planet to the particle, ϑ represents the argument of the latitude, h accounts for the right ascension of the node while R, G and H are the conjugate momenta of r, ϑ and h respectively, see more details in [15]. Also, the action G represents the modulus of the angular momentum vector, i.e. $G = |\mathbf{G}| = |\mathbf{x} \times \mathbf{P}|$ and $H = x P_y - y P_x$ stands for the third component of the angular momentum, that is, $H = P_\phi$. We notice that $0 \leq |H| \leq G$. The inclination of the orbital plane with respect to the equatorial plane is defined by the angle I such that $\cos I = H/G$, where I is defined on $[0, \pi]$. These coordinates are singular for $r = 0, G = 0$ and $G = |H|$. The condition $|H| < G$ ensures that I is defined properly in $(0, \pi)$ and that $\mathbf{G}$ is not parallel to the z axis, so h is well defined. Thus, polar-nodal coordinates are not valid for rectilinear and equatorial trajectories.

The second set of coordinates is the so called Delaunay coordinates and are given by (ℓ, g, h, L, G, H). The angle ℓ refers to the mean anomaly, g is the argument of the pericentre and L the square of the semimajor axis, hence $0 \leq |H| \leq G \leq L$. The condition $G < L$ ensures that the ellipse does not degenerate to a circle, thus g and ℓ are well defined and $|H| < G$ ensures that h is well defined. Thus, Delaunay coordinates present singularities for rectilinear, circular and equatorial trajectories, see details in [15,16]. However, circular and equatorial singularities can be handled by an appropriate combination of Delaunay elements [17], as will be done to study these particular types of motion later.

Both polar-nodal and Delaunay coordinates are symplectic. Typically, the Hamiltonian $\mathcal{H}'$ is expressed as a combination of polar-nodal and Delaunay elements. We denote the resulting Hamiltonian by the same expression $\mathcal{H}'$. According to the discussion made in Section 2 we consider the potentials U_e, U_m and U_{J_2} to be of the same order and much smaller than U_K. Thus we treat the problem as a perturbed Kepler Hamiltonian, splitting $\mathcal{H}'$ as the sum of the pure Kepler problem $\mathcal{H}'_0$ plus the first-order perturbation that takes into account the potential related to the electrostatic and magnetic fields as well as the gravitational contribution of the oblateness of the planet.

Now, the method of averaging, which in the context of Kepler system is called the normalisation of Delaunay, may be interpreted as a change of coordinates that allows us to pass from $\mathcal{H}'$ to a new Hamiltonian $\mathcal{K}$ averaging (normalising) over the mean anomaly. Proceeding only to first order, we make

$$\mathcal{H}'_0 = \frac{1}{2}\left(P_\rho^2 + P_z^2 + \frac{P_\phi^2}{\rho^2}\right) - \frac{1}{r} = -\frac{1}{2L^2}, \qquad \mathcal{H}'_1 = \mathcal{H}' - \mathcal{H}'_0.$$

Next, we identify $\mathcal{K}_0$ with $\mathcal{H}'_0$ and try to solve the homological equation

$$\frac{1}{L^3}\frac{\partial \mathcal{W}_1}{\partial \ell} + \mathcal{K}_1 = \mathcal{H}'_1.$$

The solution of this is the pair $(\mathcal{K}_1, \mathcal{W}_1)$, where $\mathcal{K}_1$ corresponds with the average with respect to the mean anomaly

$$\mathcal{K}_1 = (2\pi)^{-1}\int_0^{2\pi} \mathcal{H}'_1 \, d\ell,$$

whereas $\mathcal{W}_1$ is the associated generated function. It is a periodic function of ℓ, g and h and is explicitly calculated through the integral

$$\mathcal{W}_1 = L^3\left(\int \mathcal{H}'_1 \, d\ell - \mathcal{K}_1 \, \ell\right).$$

This averaging process is performed in the framework of Lie transformations [18]. After performing the computations we arrive at the Hamiltonian

$$\mathcal{K} = \mathcal{K}_0 + \mathcal{K}_1, \tag{5}$$

with

$$\mathcal{K}_0 = -\frac{1}{2\,L^2},$$

$$\mathcal{K}_1 = \frac{\delta}{16\,L^5\,G^7\,(L+G)}\Big(2\,(L+G)\,\big(4\,\beta\,L^3\,G^7 + 4\,\beta\,L^3\,G^5\,H^2 - \delta\,G^4 - 8\,L^2\,G^4\,H - \delta\,G^2\,H^2 + 3\,\delta\,L^2\,G^2 + 3\,\delta\,L^2\,H^2\big) + (L-G)\,(G^2-H^2)\,\big(8\,\beta\,L^3\,G^5 + \delta\,G^2 + 2\,\delta\,L\,G + \delta\,L^2\big)\,\cos(2\,g)\Big) + \frac{J_2\,(G^2-3\,H^2)}{4\,L^3\,G^5}.$$

The associated generating function is given by $\mathcal{W}_1$ with

$$\begin{aligned}\mathcal{W}_1 = {} & \frac{\delta}{48\,L^2\,G^7\,(L^2-G^2)\,r^2}\Big(6\,(L^2-G^2)\,r^3\,\big(-8\,L^2\,G^4\,H\,\varphi\,r - \delta\,G^4\,\varphi\,r - \delta\,G^2\,H^2\,\varphi\,r + 3\,\delta\,L^2\,G^2\,\varphi\,r + 3\,\delta\,L^2\,H^2\,\varphi\,r \\ & + \delta\,L^2\,G^5\,R + \delta\,L^2\,G^3\,H^2\,R - 8\,L^2\,G^5\,H\,r\,R + 3\,\delta\,L^2\,G^3\,r\,R + 3\,\delta\,L^2\,G\,H^2\,r\,R + 4\,\beta\,L^2\,G^7\,r^2\,R \\ & + 4\,\beta\,L^2\,G^5\,H^2\,r^2\,R\big) + (G^2-H^2)\,r\,\big(-48\,\beta\,L^4\,G^6\,\varphi\,r^3 + 3\,\delta\,G^4\,\varphi\,r^3 - 6\,\delta\,L^2\,G^2\,\varphi\,r^3 + 3\,\delta\,L^4\,\varphi\,r^3 + 6\,\delta\,L^4\,G^7\,R \\ & - 2\,\delta\,L^4\,G^5\,r\,R - 3\,\delta\,L^2\,G^5\,r^2\,R + \delta\,L^4\,G^3\,r^2\,R + 48\,\beta\,L^4\,G^7\,r^3\,R - 5\,\delta\,L^2\,G^3\,r^3\,R + 3\,\delta\,L^4\,G\,r^3\,R \\ & + 24\,\beta\,L^2\,G^7\,r^4\,R + 24\,\beta\,L^4\,G^5\,r^4\,R\big)\,\cos(2\,g) + 2\,L^4\,G^6\,(G^2-H^2)\,\big(3\,\delta\,G^2 - 4\,\delta\,r + 24\,\beta\,G^2\,r^3 \\ & - 24\,\beta\,r^4\,\log(G^2/r)\big)\,\sin(2\,g)\Big) + \frac{J_2}{4\,G^5\,(L^2-G^2)\,r^3} \times \Big((L^2-G^2)\,(G^2-3\,H^2)\varphi\,r^3 \\ & + G\,(L^2-G^2)\,(G^2-3\,H^2)\,r^3\,R + G^3\,(G^2-H^2)\,(r^2-L^2\,r-2\,L^2\,G^2)\,r\,R\,\cos(2\,g) \\ & + L^2\,G^4\,(G^2-H^2)\,(3\,r-2\,G^2)\,\sin(2\,g)\Big),\end{aligned}$$

where $\varphi = f - \ell, f$ is the angle called the true anomaly and φ is the angle called the equation of the centre, see for instance [16]. In the computations we have avoided using Fourier expansions in the angular variables and power expansions in the eccentricity of the trajectories, as is the usual procedure in celestial mechanics. So, by combining polar-nodal with Delaunay coordinates and making use of the angle φ we get compact expressions that are valid for any type of elliptic motion.

It can be proved that the generating function $\mathcal{W}_1$ is well defined for circular motions for which $e = 0$ (equivalently $G = L$), although it is not obvious. This can be achieved by expressing the variables that depend upon G in terms of it, that is, the variables r, R and φ, and showing that the limit of $\mathcal{W}_1$ when G tends to L is bounded.

The normalisation of Delaunay is symplectic, thus the resulting Hamiltonian $\mathcal{K}$ is given in the transformed (new) coordinates, but we use the same names for all the coordinates in order to simplify notation. Moreover, the generating function is used to express the new coordinates in terms of the old ones or vice versa. For instance, the old action L is given in terms of the new variables by means of $L - \partial\,\mathcal{W}_1/\partial\ell$ + higher-order terms.

Finally, we note that the formulae of $\mathcal{K}_1$ and $\mathcal{W}_1$ coincide with those of the paper [4, p. 248] after setting $J_2 = 0$.

4. Reductions and reduced phase spaces

4.1. Reductions by continuous symmetries

Once the higher-order terms are dropped, the action $L > 0$ is an integral of motion that can be fixed. Thus, the normalised Hamiltonian $\mathcal{K}$ defines a system of two degrees of freedom on a four-dimensional phase space. This space, called the first-reduced phase space, has been studied by many authors, see for instance [19,20]. It is the product of the two-spheres

$$S_L^2 \times S_L^2 = \Big\{(\mathbf{a},\mathbf{b}) \in \mathbb{R}^6 \mid a_1^2 + a_2^2 + a_3^2 = L^2,\, b_1^2 + b_2^2 + b_3^2 = L^2\Big\},$$

where $(\mathbf{a},\ \mathbf{b}) \equiv (\mathbf{G} + L\,\mathbf{A}_L,\ \mathbf{G} - L\,\mathbf{A}_L)$ and $\mathbf{A}_L$ is the Laplace–Runge–Lenz vector defined by

$$\mathbf{A}_L = \mathbf{P} \times \mathbf{G} - \frac{\mathbf{x}}{\|\mathbf{x}\|}.$$

Now we need to put Hamiltonian (5) in terms of **a** and **b**. Since $\mathcal{K}_0$ is constant, we drop it and work with $\mathcal{K}_1$, writing it in terms of the coordinates of $S_L^2 \times S_L^2$. The result is a Hamiltonian called the first-reduced Hamiltonian and it is a rational function of **a** and **b**. The condition $G = 0$ viewed in terms of **a** and **b** means that $\mathbf{b} = -\mathbf{a}$. It implies that the first-reduced Hamiltonian has a pole when $\mathbf{b} = -\mathbf{a}$. However, equatorial ($G = |H|$) and circular ($G = L$) trajectories, which are not defined in Delaunay variables, are contained in $S_L^2 \times S_L^2$ and can be analysed properly. This follows from the fact that the process of normalisation carried out in a different set of variables, free of singularities, gives rise to the same system [21], and the singularities disappear when changed to appropriate variables. Also, if a certain Hamiltonian independent of ℓ is well defined for $G = 0$, its related reduced Hamiltonian is well defined on $S_L^2 \times S_L^2$.

The fact that P_ϕ is an integral of motion of Hamiltonian $\mathcal{H}$ is inherited through the averaging process, thus H is an integral of $\mathcal{K}$. We can reduce the first-reduced Hamiltonian by the symmetry introduced by H. If we denote $\tau = (\tau_1, \tau_2, \tau_3)$, we can define the mapping

$$\begin{aligned}\pi_H : S_L^2 \times S_L^2 &\longrightarrow \{H\} \times \mathbb{R}^3 \\ (\mathbf{a},\mathbf{b}) &\mapsto (H, \tau_1, \tau_2, \tau_3) \equiv (H, \tau),\end{aligned}$$

where

$$\tau_1 = \frac{1}{2}\,(a_3 - b_3), \qquad \tau_2 = a_1\,b_2 - a_2\,b_1, \qquad \tau_3 = a_1\,b_1 + a_2\,b_2. \tag{6}$$

After fixing both L and H, the corresponding phase space, called the twice-reduced phase space and denoted by $\mathcal{T}_{L,H}$, is defined as the image of the product $S_L^2 \times S_L^2$ by π_H, that is,

$$\begin{aligned}\mathcal{T}_{L,H} &= \pi_H(S_L^2 \times S_L^2) \\ &= \Big\{\tau \in \mathbb{R}^3 \mid \tau_2^2 + \tau_3^2 = \Big((L+\tau_1)^2 - H^2\Big) \times \Big((L-\tau_1)^2 - H^2\Big)\Big\},\end{aligned} \tag{7}$$

for $0 \le |H| \le L$ and $L > 0$. Note that τ_2 and τ_3 always belong to the interval $[H^2 - L^2, L^2 - H^2]$, whereas τ_1 belongs to $[|H| - L, L - |H|]$.

In Refs. [20,22] it is proved that if $0 < |H| < L$, $\mathcal{T}_{L,H}$ is diffeomorphic to the two-sphere S^2 and therefore the reduction is regular in that region of the phase space. However, when $H = 0$ the surface $\mathcal{T}_{L,0}$ is a topological two-sphere with two singular points: the vertices at $(\pm L, 0, 0)$, giving rise to the concept of singular reduction. The reason for the existence of these two points is that the S^1-action related to the axial symmetry reduction has two fixed points: $L\,(\pm 1, 0, 0, \mp 1, 0, 0)$ and consequently this action is not free. Finally, when $|H| = L$ the phase space $\mathcal{T}_{L,\pm L}$ gets reduced to a point.

It is not difficult to prove that Delaunay variables not involving the angles ℓ and h can be expressed in terms of τ. In particular we get

$$G^2 = \frac{1}{2}(L^2 + H^2 - \tau_1^2 + \tau_3),$$
$$\cos g = \frac{-\tau_2}{\sqrt{(L^2 - H^2)^2 - (\tau_1^2 - \tau_3)^2}}, \tag{8}$$
$$\sin g = \tau_1 \sqrt{\frac{2(L^2 + H^2 - \tau_1^2 + \tau_3)}{(L^2 - H^2)^2 - (\tau_1^2 - \tau_3)^2}}.$$

Using these relations it is possible to express the quantities $\sin I, \cos I, \sin g, \cos g$ and G in terms of τ, L and H. Also, the eccentricity e can be put in terms of the integrals L and H through the variable G, see [23].

Circular type solutions are concentrated on a unique point of $\mathcal{T}_{L,H}$ with coordinates $(0, 0, L^2 - H^2)$ – or on a unique point of $\mathcal{T}_{L,0}$ with coordinates $(0, 0, L^2)$ – whereas equatorial trajectories in this twice-reduced phase space are represented in the negative extreme point of $\mathcal{T}_{L,H}$ with coordinates $(0, 0, H^2 - L^2)$ (respectively, at the point $(0, 0, -L^2)$ of $\mathcal{T}_{L,0}$). Thus, both types of motion can be properly treated on the space $\mathcal{T}_{L,H}$. Rectilinear trajectories could be handled as well if a particular Hamiltonian in Delaunay coordinates independent of ℓ and h were well defined for $G = 0$, but it is not the case for the Hamiltonian we tackle in this paper.

We can write the corresponding Hamiltonian (the so called twice-reduced Hamiltonian) in terms of the τ_i, using the formulae given in (8). After dropping constant terms, we end up with a rational function of τ and the parameters δ, β, J_2, L and H. It defines a one-degree-of-freedom system, with L and H as two independent integrals, given by the expression

$$\mathcal{M} = \frac{\delta}{4\sqrt{2}L^5\tau_4^7(\tau_4 + \sqrt{2}L)^2}\Big(-\delta(\tau_4 + \sqrt{2}L)^2\big(\tau_4^2(3\tau_4^2 + 4\tau_1^2 - 14L^2) + 2H^2(\tau_4^2 - 10L^2)\big) + 8L^2\tau_4^4\big(-2H(\tau_4 + \sqrt{2}L)^2 + \beta L\tau_4^2(L\tau_4^2 - \sqrt{2}\tau_4(\tau_1^2 - L^2 - H^2) + 2LH^2)\big)\Big) + \frac{J_2(2\tau_4^2 - 3H^2)}{16\sqrt{2}L^3\tau_4^5},$$

where $\tau_4 = \sqrt{L^2 + H^2 - \tau_1^2 + \tau_3}$.

4.2. Fully-reduced phase spaces and fully-reduced Hamiltonian

Now we consider the discrete symmetries of the departure system. The generators of the group of discrete symmetries of $\mathcal{H}$ are

$$\mathcal{R}_1 : (x, y, z, P_x, P_y, P_z) \longrightarrow (x, -y, -z, -P_x, P_y, P_z),$$
$$\mathcal{R}_2 : (x, y, z, P_x, P_y, P_z) \longrightarrow (x, -y, z, -P_x, P_y, -P_z).$$

These symmetries are anti-symplectic reflections and time-reversing symmetries, so if $(x(t), y(t), z(t), P_x(t), P_y(t), P_z(t))$ is a solution, then so are $(x(-t), -y(-t), \pm z(-t), -P_x(-t), P_y(-t), P_z(-t))$. The fixed-points sets of these two symmetries are Lagrangian subplanes, i.e.

$$\mathcal{L}_1 = \{(x, 0, 0, 0, P_y, P_z)\}, \qquad \mathcal{L}_2 = \{(x, 0, z, 0, P_y, 0)\}$$

are fixed by the symmetries $\mathcal{R}_1$ and $\mathcal{R}_2$, see also [24].

The symmetries $\mathcal{R}_1$ and $\mathcal{R}_2$ are conserved through the two previous reductions. In particular the twice-reduced Hamiltonian depends explicitly on τ_1^2 and on τ_3 but it is independent of τ_2, enjoying the discrete symmetries

$$\mathcal{R}_1 : (\tau_1, \tau_2, \tau_3) \longrightarrow (-\tau_1, \tau_2, \tau_3),$$
$$\mathcal{R}_2 : (\tau_1, \tau_2, \tau_3) \longrightarrow (\tau_1, -\tau_2, \tau_3).$$

In this way, if the phase flow is known for $\tau_1 \geq 0$ and $\tau_2 \geq 0$ it can be extended, by virtue of discrete symmetries $\mathcal{R}_1$ and $\mathcal{R}_2$, to the whole twice-reduced phase space. Taking this into account, we can introduce a fully-reduced system in the orbit space generated by the action of the two symmetries. Similarly to Cushman and Sadovskií [25] we define the orbit map $\mathbf{R}^3 \to \mathbf{R}^2 : (\tau_1, \tau_2, \tau_3) \to (\sigma_1, \sigma_2)$, where

$$\sigma_1 = (L - |H|)^2 - \tau_1^2, \qquad \sigma_2 = \frac{\sqrt{L^2 + H^2 - \tau_1^2 + \tau_3}}{\sqrt{2}}. \tag{9}$$

The variable σ_1 is related to the argument of pericentre g and σ_2 is the modulus of the angular momentum vector, i.e. $\sigma_2 = G$. We have that the constraints between the new variables are deduced from the constraint of (7):

(i) $|H| > 0$: the fully-reduced phase space $\mathcal{U}_{L,H}$ is bounded by the curves

$$\sigma_1\sigma_2^2 = (\sigma_2^2 - L|H|)^2, \quad \sigma_1 = (L - |H|)^2, \tag{10}$$

(ii) $H = 0$: the fully-reduced phase space $\mathcal{U}_{L,0}$ is bounded by

$$\sigma_1 = \sigma_2^2, \qquad \sigma_2 = 0, \qquad \sigma_1 = L^2. \tag{11}$$

More details on the spaces $\mathcal{U}_{L,H}$ and the reduction procedure appears in [4,10].

Next, the averaged Hamiltonian $\mathcal{K}$ (or the twice-reduced Hamiltonian $\mathcal{M}$) needs to be expressed in terms of σ_1 and σ_2. Using the inverse of (9), which puts τ_1^2 and τ_3 in terms of σ_1 and σ_2 and dropping constant terms, $\mathcal{M}$ is transformed into the so called fully-reduced Hamiltonian that results in

$$\mathcal{V} = \frac{\delta}{16L^5\sigma_2^7(\sigma_2 + L)^2}\Big(-\delta(\sigma_2 + L)^2\big(3\sigma_2^4 - (2\sigma_1 + 5L^2 + 4L|H| - 3H^2)\sigma_2^2 - 5L^2H^2\big) + 16L^2\sigma_2^4\big(\beta L^2\sigma_2^4 + \beta L(\sigma_1 + 2L|H|)\sigma_2^3 + H(\beta L^2H - 1)\sigma_2^2 - 2LH\sigma_2 - L^2H\big)\Big) + \frac{J_2(\sigma_2^2 - 3H^2)}{4L^3\sigma_2^5}. \tag{12}$$

The Hamiltonian $\mathcal{V}$ is well defined on $\mathcal{U}_{L,H}$ for $|H| > 0$ as then $\sigma_2 \geq |H|$ cannot reach the value zero. However, when $H = 0$, $\mathcal{V}$ is not bounded for σ_2 from below. Thus, in this case we fix a minimum value of σ_2, say G^*, such that σ_2 is bounded in $[G^*, L]$. We note that it is not possible to get rid of the singularity at $\sigma_2 = 0$ (when $H = 0$) as it is inherited from the singularity at $r = 0$ that appears in (4) and that cannot be removed using regularisation or an equivalent approach. Physically we are discarding collisions of the particle with the planet. Nevertheless our approach is global in the sense that we consider all possible realistic types of motions, excepting collisions.

5. Relative equilibria and bifurcations

5.1. Equilibrium points

Equilibrium points in the twice-reduced phase space $\mathcal{T}_{L,H}$ can be obtained by zeroing the corresponding equations of motion or taking into account that the flow is generated by the intersection of the family of surfaces defined by $\mathcal{M}$ and $\mathcal{T}_{L,H}$. Due to the symmetries $\mathcal{R}_1$ and $\mathcal{R}_2$, if $E \equiv (\tau_1, \tau_2, \tau_3)$ is an equilibrium point, also are equilibrium points

$$(-\tau_1, \tau_2, \tau_3), \qquad (\tau_1, -\tau_2, \tau_3), \qquad (-\tau_1, -\tau_2, \tau_3).$$

In this sense, if we study the equilibria of the fully-reduced system, in the orbit space $\mathcal{U}_{L,H}$, we avoid this multiplicity, in such a way that a critical point in the interior of $\mathcal{U}_{L,H}$ corresponds to four critical points in $\mathcal{T}_{L,H}$, a critical point in the boundary of $\mathcal{U}_{L,H}$ corresponds to two critical points in $\mathcal{U}_{L,H}$ and only the points

$$((L-|H|)^2,\ |H|), \qquad ((L-|H|)^2,\ L),$$

correspond to a single critical point in $\mathcal{T}_{L,H}$, namely $(0, 0, L^2 - H^2)$ and $(0, 0, H^2 - L^2)$, which represent the class of equatorial and circular motions respectively, provided $H \neq 0$. Moreover, the equilibria of $\mathcal{V}$ can be obtained through the relative and absolute extrema of $\mathcal{V}$ on $\mathcal{U}_{L,H}$. As $\mathcal{V}$ is a rational function of σ_1 and σ_2, the problem of finding the equilibrium points can be reduced to that of finding roots of a polynomial.

In the same way as in [4] we neglect those terms in δ^2 in (12) because their contribution is small compared with the rest of the terms. Thus, we are concerned with the equilibrium points of the Hamiltonian

$$\mathcal{Z} = \frac{\delta\left(\beta L \sigma_2^2 \left(\sigma_1 \sigma_2 + L(\sigma_2 + |H|)^2\right) - H(L+\sigma_2)^2\right)}{L^3 \sigma_2^3 (\sigma_2 + L)^2} + \frac{J_2(\sigma_2^2 - 3H^2)}{4L^3\sigma_2^5}. \tag{13}$$

We note that $\mathcal{Z}$ is a scalar function depending on two variables, σ_1 and σ_2, defined on a bounded subset of $\mathbb{R}^2$, which is continuous in $\mathcal{U}_{L,H}$ when $|H| > 0$ whereas for $H = 0$ it is continuous provided that we fix $G^* > 0$ such that $G^* \leq \sigma_2 \leq L$. Thus we assure continuity of $\mathcal{Z}$ if we remove the part of the space $\mathcal{U}_{L,0}$ such that $0 \leq \sigma_2 < G^*$.

The situation is a bit more complex than the one in [4] because δ is not a common factor in $\mathcal{Z}$ and must be taken into account, as well as the rest of the parameters. Hence, two extra parameters appear in contrast to the case discussed in [4]: δ, the charge–mass ratio of the particle, and J_2, the oblateness of the planet. The relative size of them will lead to different situations, which gives an idea of the complex dynamics of the problem.

Equilibria are determined by the extremum points of (13) on the reduced space $\mathcal{U}_{L,H}$. To begin with, we note that the extremum points on the boundary of the fully-reduced phase space,

$$E_1 \equiv \left((L-|H|)^2,\ |H|\right) \quad \text{and} \quad E_2 \equiv \left((L-|H|)^2,\ L\right),$$

are always equilibria provided that $|H| > 0$, as $\mathcal{Z}$ is a continuous function in $\mathcal{U}_{L,H}$ for $|H| > 0$. This conclusion can also be extracted by going back to the formulation of the system in $\mathcal{T}_{L,H}$. The point E_1 accounts for the set of equatorial motions whereas E_2 corresponds to the circular solutions. When $H = 0$, the point E_1 is not in the region of $\mathcal{U}_{L,H}$ where $\mathcal{Z}$ is continuous but E_2 remains as an equilibrium point.

To account for the remaining equilibria we compute the partial derivatives $\partial\mathcal{Z}/\partial\sigma_1$ and $\partial\mathcal{Z}/\partial\sigma_2$. The expression for $\partial\mathcal{Z}/\partial\sigma_1$,

$$\frac{\partial \mathcal{Z}}{\partial \sigma_1} = \frac{\delta\beta}{L^2(\sigma_2+L)^2},$$

does not depend on J_2 and the situation is similar to that discussed in [4]. In general, $\partial\mathcal{Z}/\partial\sigma_1$ does not vanish and, consequently, the function $\mathcal{Z}$ cannot have any critical point in the interior of $\mathcal{U}_{L,H}$. However, if the particle is not charged ($\delta = 0$), $\partial\mathcal{Z}/\partial\sigma_1$ vanishes identically. By computing the other partial derivative we arrive at

$$\frac{\partial \mathcal{Z}}{\partial \sigma_2} = -\frac{3J_2(\sigma_2^2 - 5H^2)}{4L^3\sigma_2^6},$$

recovering the well known case of the critical inclination for the main problem of an artificial satellite [20,26]. In addition to the two equilibrium points E_1 and E_2, a nonisolated set of equilibria appears for $\sigma_2 = \sqrt{5}\,|H|$, provided that $\sqrt{5}\,|H| \leq L$.

When the particle is charged ($\delta \neq 0$), $\partial\mathcal{Z}/\partial\sigma_1$ does not vanish for any value of σ_2 and, consequently, the remaining possible equilibria are located on the boundary of $\mathcal{U}_{L,H}$.

Similarly to how we proceeded in [4], in order to analyse these equilibria, two cases must be considered:

(a) those equilibria located on the rectilinear part of the boundary given by the curve $\sigma_1 = (L-|H|)^2$, under the restriction $|H| \leq \sigma_2 \leq L$;
(b) those equilibria located on the curved part of the boundary defined by $\sigma_1\sigma_2^2 = (\sigma_2^2 - L|H|)^2$ and $|H| \leq \sigma_2 \leq L$.

For the bifurcation manifolds we use the same notation as in [4] in order to facilitate the identification of changes in the bifurcation plane.

5.1.1. Case (a)

If $\sigma_1 = (L-|H|)^2$ then (13) turns into the single real-valued function

$$\mathcal{Z}(\sigma_2) = \frac{\delta\left(\beta L(L\sigma_2^3 + H^2\sigma_2^2) - H(\sigma_2+L)\right)}{L^3\sigma_2^3(\sigma_2+L)} + \frac{J_2(\sigma_2^2 - 3H^2)}{4L^3\sigma_2^5}, \tag{14}$$

where $|H| \leq \sigma_2 \leq L$.

The extremum values are reached at $\sigma_2 = |H|$, $\sigma_2 = L$ (which are always equilibria, as we already know) and at those points satisfying

$$\frac{d\mathcal{Z}(\sigma_2)}{d\sigma_2} = \frac{\delta\left(3H(L+\sigma_2)^2 - \beta L\sigma_2^2(L\sigma_2^2 + 2H^2\sigma_2 + LH^2)\right)}{L^3\sigma_2^4(\sigma_2+L)^2} - \frac{3J_2(\sigma_2^2 - 5H^2)}{4L^3\sigma_2^6} = 0.$$

In this case σ_2 must be a root of the polynomial

$$\mathcal{P}(\sigma_2) = 4\sigma_2^2\delta\left(3H(\sigma_2+L)^2 - \beta L\sigma_2^2(L\sigma_2^2 + 2H^2\sigma_2 + LH^2)\right) - 3J_2(\sigma_2^2 - 5H^2)(\sigma_2+L)^2$$

in the interval $(|H|, L)$.

Polynomial $\mathcal{P}(\sigma_2)$ is of degree six in σ_2, thus it is not possible to derive explicitly the coordinates of the equilibria. Nevertheless, we satisfy ourselves by studying the changes in the number of roots. They will determine the bifurcation manifolds in the space of parameters. The changes in the number of roots will come from three facts:

(i) There is a root of $\mathcal{P}(\sigma_2)$: $\sigma_2^* \in (|H|, L)$, that reaches the value L. Then, the following equation must be satisfied:

$$\Gamma_1 \equiv \delta L^2(\beta L^4 + 3\beta L^2 H^2 - 12H) + 3J_2(L^2 - 5H^2) = 0.$$

(ii) There is a root of $\mathcal{P}(\sigma_2)$: $\sigma_2^* \in (|H|, L)$, that reaches the value $|H|$. Then, the following equation must be satisfied

$$\Gamma_2 \equiv -\delta H\left(2\beta L H^3 - 3(L+|H|)\right) + 3J_2(L+|H|) = 0.$$

(iii) There is a value of σ_2: $\sigma_2^* \in (|H|, L)$, such that it is a multiple root of $\mathcal{P}(\sigma_2)$. This situation takes place when the discriminant of $\mathcal{P}(\sigma_2)$ is zero. The discriminant is a polynomial in H, L, J_2, δ, β, which we do not write down here for simplicity, and gives rise to a bifurcation manifold that we denote by Γ_0.

It is worth noting that if $\delta > 0$ along the manifold Γ_0 no collision takes place between roots of $\mathcal{P}(\sigma_2)$ in the interval $[|H|, L]$.

5.1.2. Case (b)

If $\sigma_1\,\sigma_2^2 = (\sigma_2^2 - L\,|H|)^2$, Hamiltonian (13) turns into the single real valued function

$$\mathcal{Z}(\sigma_2) = \frac{\delta\left(\beta\,L\,\sigma_2\,(\sigma_2^3 + L\,H^2) - H\,(\sigma_2 + L)\right)}{L^3\,\sigma_2^3\,(\sigma_2 + L)} + \frac{J_2\,(\sigma_2^2 - 3\,H^2)}{4\,L^3\,\sigma_2^5}, \tag{15}$$

with $|H| \le \sigma_2 \le L$.

As in the previous case, $\sigma_2 = |H|$ and $\sigma_2 = L$ are extremum values and the rest are obtained from

$$\frac{d\mathcal{Z}(\sigma_2)}{d\sigma_2} = \frac{\delta\left(3\,H\,(\sigma_2 + L)^2 + \beta\,L^2\,\sigma_2\,(\sigma_2^3 - 2\,L\,H^2 - 3\,H^2\,\sigma_2)\right)}{L^3\,\sigma_2^4\,(\sigma_2 + L)^2} - \frac{3\,J_2\,(\sigma_2^2 - 5\,H^2)}{4\,L^3\,\sigma_2^6} = 0.$$

This equation is satisfied if σ_2 is a root of the degree six polynomial

$$\mathcal{Q}(\sigma_2) = -4\,\delta\,\sigma_2^2\left(3\,H\,(\sigma_2 + L)^2 + \beta\,L^2\,\sigma_2\,(\sigma_2^3 - 3\,H^2\,\sigma_2 - 2\,L\,H^2)\right) + 3\,J_2\,(\sigma_2 + L)^2\,(\sigma_2^2 - 5\,H^2).$$

The changes in the number of roots will take place, as in the case (a), in these situations:

(i) There is a root of $\mathcal{Q}(\sigma_2)$: $\sigma_2^- \in (|H|, L)$, that reaches the value $|H|$. Then, the following equation must be satisfied:

$$\Gamma_3 \equiv \delta\,H\left(2\,\beta\,L^2\,H\,|H| - 3\,(L + |H|)\right) - 3\,J_2\,(L + |H|) = 0.$$

(ii) There is a root of $\mathcal{Q}(\sigma_2)$: $\sigma_2^- \in (|H|, L)$, that reaches the value L. Then, the following equation must be satisfied:

$$\Gamma_4 \equiv -\delta\,L^2\left(\beta\,L^2\,(L^2 - 5\,H^2) + 12\,H\right) + 3\,J_2\,(L^2 - 5\,H^2) = 0.$$

(iii) There is a value of σ_2: $\sigma_2^- \in (|H|, L)$, such that it is a multiple root of $\mathcal{Q}(\sigma_2)$. This situation takes place when the discriminant of $\mathcal{Q}(\sigma_2)$ is zero. The discriminant, which we do not write here for simplicity, gives rise to a bifurcation manifold denoted by Γ_5.

We note that now, for $\delta < 0$, the third situation described above cannot occur and Γ_5 does not appear in the bifurcation diagram. In some sense the roles played by the critical points in the straight and curved parts of the boundary of $\mathcal{U}_{L,H}$ for $\delta > 0$ are interchanged when $\delta < 0$.

5.2. Bifurcation diagram

From the previous discussion it follows that, for a given planet, β and J_2 fixed, the surfaces $\Gamma_0, \ldots, \Gamma_5$, together with the constraint $|H| \le L$, divide the parameter space (H, L, δ) into different regions where the number of equilibrium points changes. In other words, the number of equilibrium solutions depends on the charge of the particle as well as on the inclination and eccentricity of the orbit.

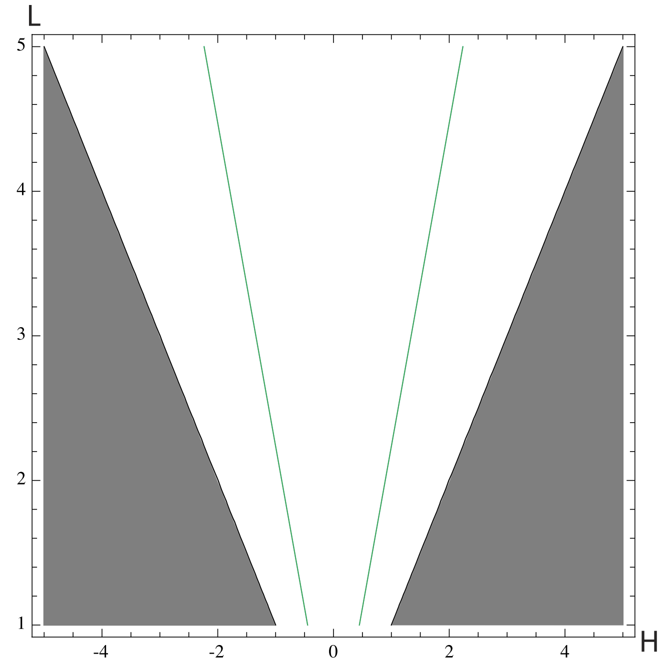

Fig. 2. The bifurcation plane (H, L) for $\delta = 0$, $\beta = 0.40649$ and $J_2 = 0.016298$.

We analyse here the particular case $\beta = 0.40649$ and $J_2 = 0.016298$, which are the ones corresponding to Saturn, by taking different slices of the surfaces of bifurcation for several values of δ. The starting point is the slice for $\delta = 0$ (see Fig. 2), the case of the main problem of an artificial satellite. Only one bifurcation appears, when the lines defined by

$$L = \sqrt{5}\,|H| \tag{16}$$

are crossed. The class of circular solutions bifurcates, giving rise to a set of nonisolated equilibria.

In fact, all the curves $\Gamma_0, \Gamma_1, \Gamma_4$ and Γ_5 reduce to (16) for $\delta = 0$. In this way, we expect that these lines evolve smoothly with δ, splitting away from the initial configuration. However, the evolution is not symmetric and different scenarios appear for positive and negative charge. This can be deduced from a remarkable fact, that the curves Γ_j $(1 \le j \le 4)$ meet in two points, which we denote by P and Q and are defined by

$$P \equiv \left\{(H, L):\; L = H > 0,\; \delta\,\beta\,L^4 - 3\,\delta\,L - 3\,J_2 = 0\right\},$$
$$Q \equiv \left\{(H, L):\; L = -H > 0,\; \delta\,\beta\,L^4 + 3\,\delta\,L - 3\,J_2 = 0\right\}.$$

It is clear that, for $\delta < 0$, the point Q cannot exist, as all the coefficients in the polynomial equation $\delta\,\beta\,L^4 + 3\,\delta\,L - 3\,J_2 = 0$ have the same sign and there is no positive root. On the other hand, if $\delta > 0$ the point Q always exists and corresponds to a retrograde circular equatorial solution. Moreover, as δ increases, the radius of the orbit tends to zero and, for values of δ greater than 0.0143532, the orbit becomes meaningless, provided its radius becomes less than one.

The point P can be present for both positive and negative charged particles. Nevertheless, while it is always present for positive charged particles, if $\delta < 0$ it must be $\delta < -0.0177175$ in order that the point P exists and $\delta < -0.0188524$, to give rise to an orbit with radius greater than one. Moreover, as the absolute value of δ increases, the point P tends to a limit position given by

$$\left(\sqrt[3]{\frac{3}{\beta}},\; \sqrt[3]{\frac{3}{\beta}}\right).$$

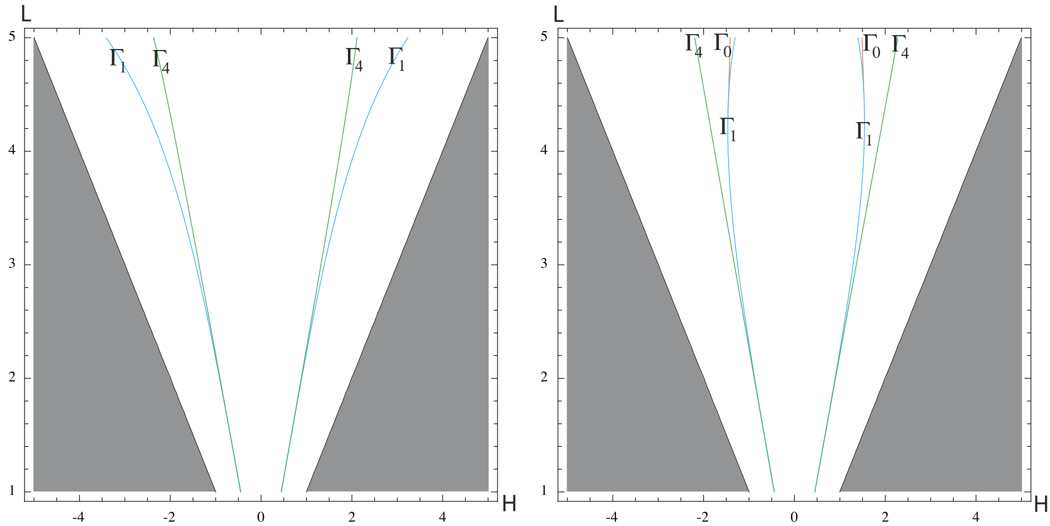

Fig. 3. The bifurcation plane (H, L) for $\delta = 0.0001$ (left) and $\delta = -0.0001$ (right), $\beta = 0.40649$ and $J_2 = 0.016298$.

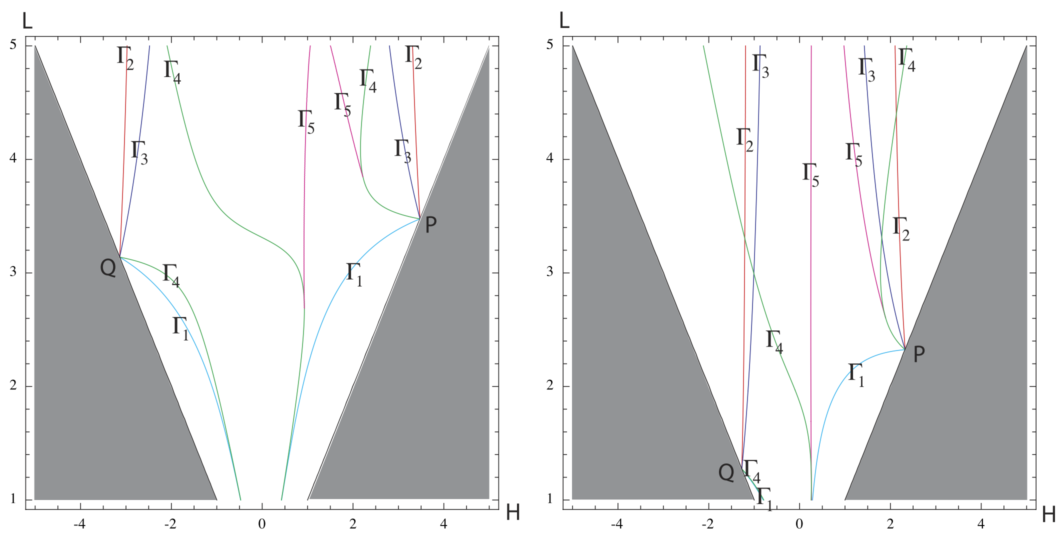

Fig. 4. The bifurcation plane (H, L) for $\delta = 0.001$ (left) and $\delta = 0.01$ (right), $\beta = 0.40649$ and $J_2 = 0.016298$.

We stress that these are the same coordinates for the point P described in [4]. So, when the effect of the oblateness is negligible, we recover the dynamics of the generalised Størmer problem studied in [4], where a rich scenario of bifurcations around P appeared. However, when the combined effect of δ and J_2 is considered, only if δ is large enough, will the point P play an important role in the dynamics of the problem, as we shall show in the following discussion.

If δ is close to zero the bifurcation diagram, restricted to orbits such that $1 < L < 5$, is very similar to that presented in Fig. 2. Only circular orbits bifurcate in the range considered, while equatorial ones remain unchanged. In terms of the sign of the particle's charge, the main difference results in the way the bifurcation lines evolve. For δ positive, the curves Γ_1 and Γ_4 evolve outwards, while for δ negative, Γ_1 evolves inwards, as it is shown in Fig. 3. It is worth noting that the points P and Q do not appear in the range considered due to the small values taken by δ. We also note the appearance of the curve Γ_0, which is tangent to Γ_1 only for negative charged particles.

As δ increases in absolute value, the bifurcation diagram becomes more intricate for positive charged particles, as is shown in Fig. 4. The points P and Q are present and most of the bifurcation lines meet there, except Γ_5, which ends when it is tangent to Γ_4. The stability analysis of the circular equatorial motions (including in particular the points P and Q) as well as the reconstruction of these motions to the original flow is done in [27].

We count sixteen different regions in the parameter plane, where different flows are obtained, commanded by the equilibrium points and their stability character. In Fig. 5, the different regions are numbered and a scheme with the critical points and their stability on the fully-reduced space $\mathcal{U}_{L,H}$ is depicted. A black dot means a linear unstable equilibrium and a white point a linear stable one. From this scheme it can be appreciated which type of bifurcation takes place every time a Γ_k line is crossed. All the lines Γ_k correspond to parametric bifurcations of pitchfork type, except Γ_5 which corresponds to a saddle-centre bifurcation. This conclusion follows from the number of equilibrium points involved in the bifurcation together with the Index Theorem and a theorem on the multiplicity of a root for a vanishing resultant. We also note that at the points where two bifurcation lines intersect, two different points of the reduced phase space bifurcate at the same time, and at the tangency points, the two bifurcations take place at the same time and at the same point.

Details on some parts of the bifurcation plane given in Fig. 5 are represented in Fig. 6.

For negative charged particles the bifurcation diagram is simpler, at least for values of $\delta \geq -0.01$. In Fig. 7, two slices for

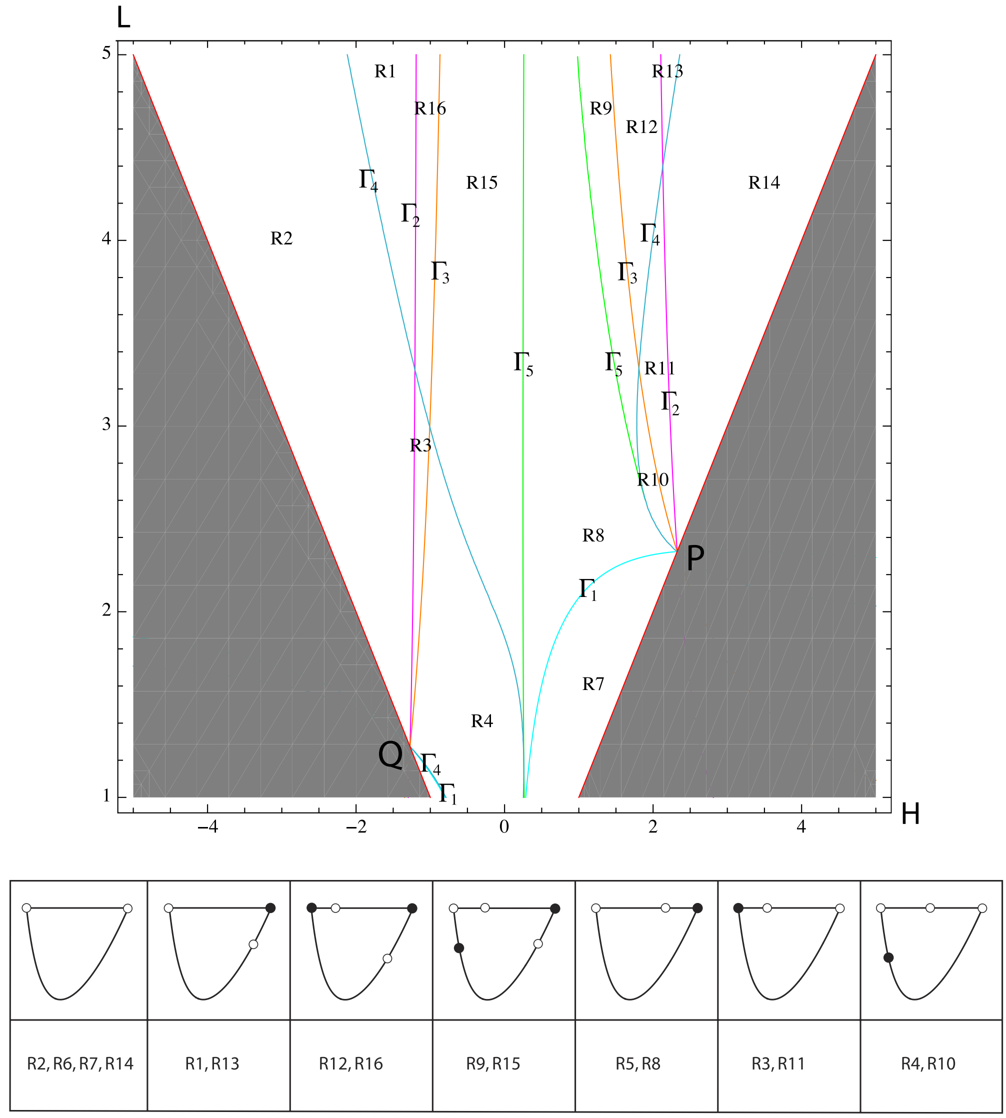

Fig. 5. The bifurcation plane (H, L) for $\delta = 0.01$, $\beta = 0.40649$ and $J_2 = 0.016298$ with the sixteen different regions it is divided into. There is a tiny region between the lines Γ_1 and Γ_4, which we call *R5*. It can be seen more clearly in Fig. 6. Below, the critical points for each region represented in the space $\mathcal{U}_{L,H}$: a black dot means instability (saddle), a white point means stability (centre). Points E_1 and E_2 appear respectively on the left and right corners of $\mathcal{U}_{L,H}$.

$\delta = -0.001$ and $\delta = -0.01$ show very few differences from the previous slice in Fig. 3. The most noticeable fact is the appearance of the closed loop for Γ_1, also present for $\delta = -0.0001$, but outside the range of L considered.

However, if δ reaches the critical value $\delta = -0.0188524$, the point P appears in the lower part of the bifurcation plane and a similar dynamics to the positive case arises. Now there are ten different regions and the flow in each region is conducted by the equilibrium points and their stability. This is shown in Fig. 8, where the different situations are accounted for. The relative equilibria and their stability are sketched on the fully-reduced space $\mathcal{U}_{L,H}$. Also, it can be seen how the saddle-centre bifurcation now takes place in the rectilinear part of the boundary of the reduced space, whereas it was in the curved part for $\delta > 0$.

As a consequence of the above discussion it can be said that particles in the vicinity of the points P and Q can suffer sudden instabilities if the charge of the particle is subject to changes due to the ambient conditions. This can be related to the spokes of Saturn. Spokes are dark radial features in the B ring which are thought to be microscopic dust particles that levitate away from the ring plane. They are shaped somewhat like an hour-glass with the narrow centres located near the synchronous orbit radius. There are several mechanisms proposed for the appearance of spokes, all of them based on more complex models than those presented here [28–31]. Recent studies of the data supplied by the Hubble Space Telescope indicate that the spokes are formed by tiny dust particles with a size of about 0.6 μm, with a very sharp distribution around this value. As we will see, in the ambient conditions of Saturn, the points P and Q are located near the synchronous orbit precisely for submicron sized particles. Indeed, assuming a spherical icy particle, δ is a function of the radius a of the particle and of the surface potential Φ given by

$$\delta = 0.00133887 \frac{\Phi}{a^2}, \tag{17}$$

see the details in [32]. As the points P and Q are functions of δ, we can obtain the specific values of them to be located exactly at the distance of the synchronous orbit. Thus, P is at the right position if $\delta \approx -0.18$, where Q is related to the synchronous orbit for $\delta = 0.01$. By inserting these values into (17) for $\Phi \in [-10, 5]$, a typical interval for Saturn (see [33]), we obtain that the size of the particle must be less than 0.9 μm, in agreement with the estimations for the size of the dust particles in the spokes. How this mechanism or

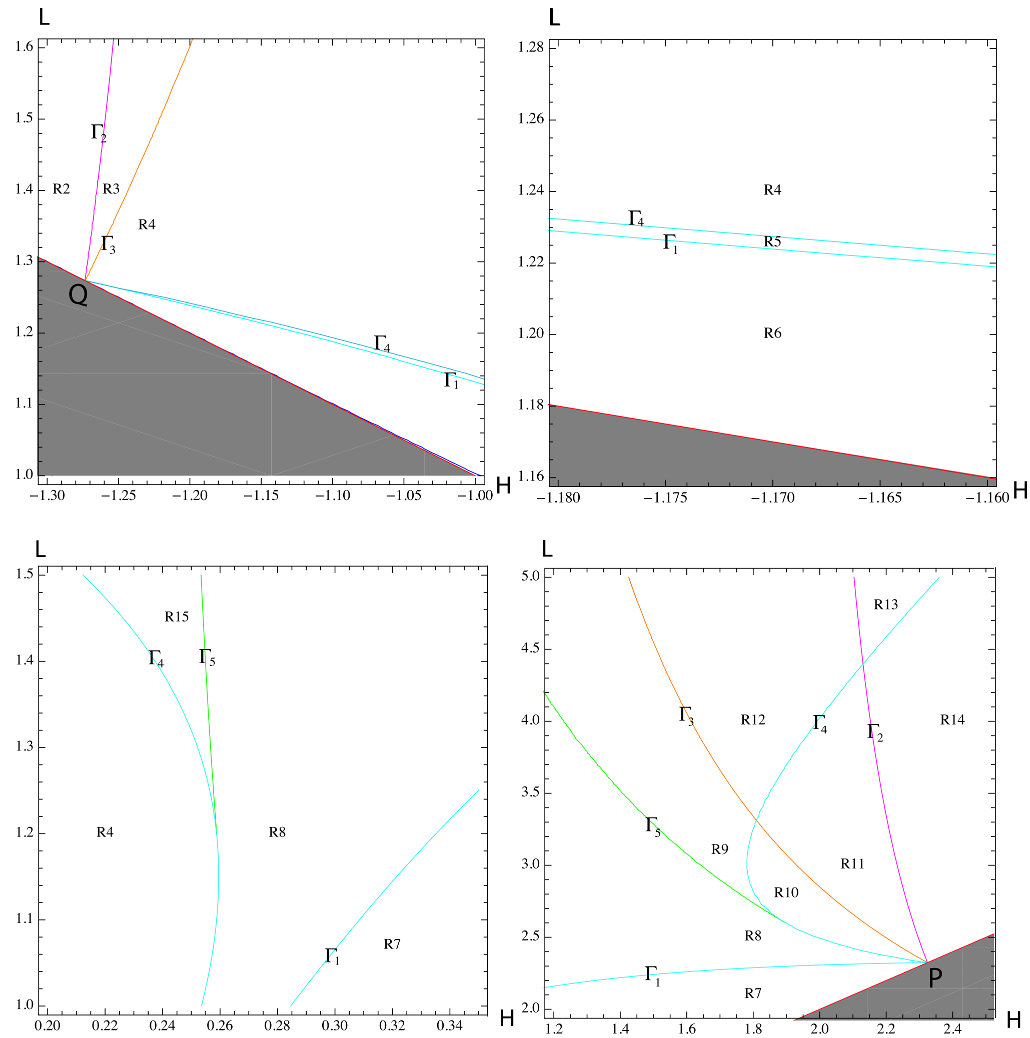

Fig. 6. Details on the bifurcation plane (H, L) of Fig. 5. The top pictures are a zoom of the left part of the plane. Bottom left picture is a zoom of the central bottom part of the plane. Bottom right picture is a zoom of the right part of the plane.

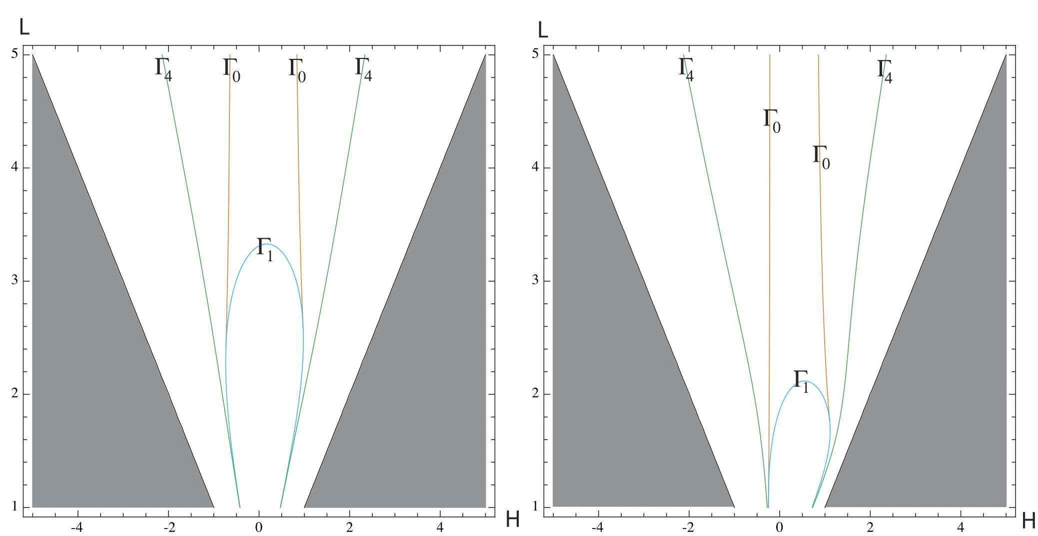

Fig. 7. The bifurcation plane (H, L) for $\delta = -0.001$ (left) and $\delta = -0.01$ (right), $\beta = 0.40649$ and $J_2 = 0.016298$.

that proposed in [5] can help in the formation of spokes deserves further analysis.

Finally, we have studied the possible occurrence of saddle-connection bifurcations between the points E_1 and E_2, as ocurred for the problem with $J_2 = 0$ and $\delta > 0$ [4]. This global bifurcation would occur if both points are saddles having the same energy and this situation takes place for $\delta > 0$ in the regions $R12$ and $R16$ and for $\delta < 0$ in the region $R6$. We have checked that for positive values

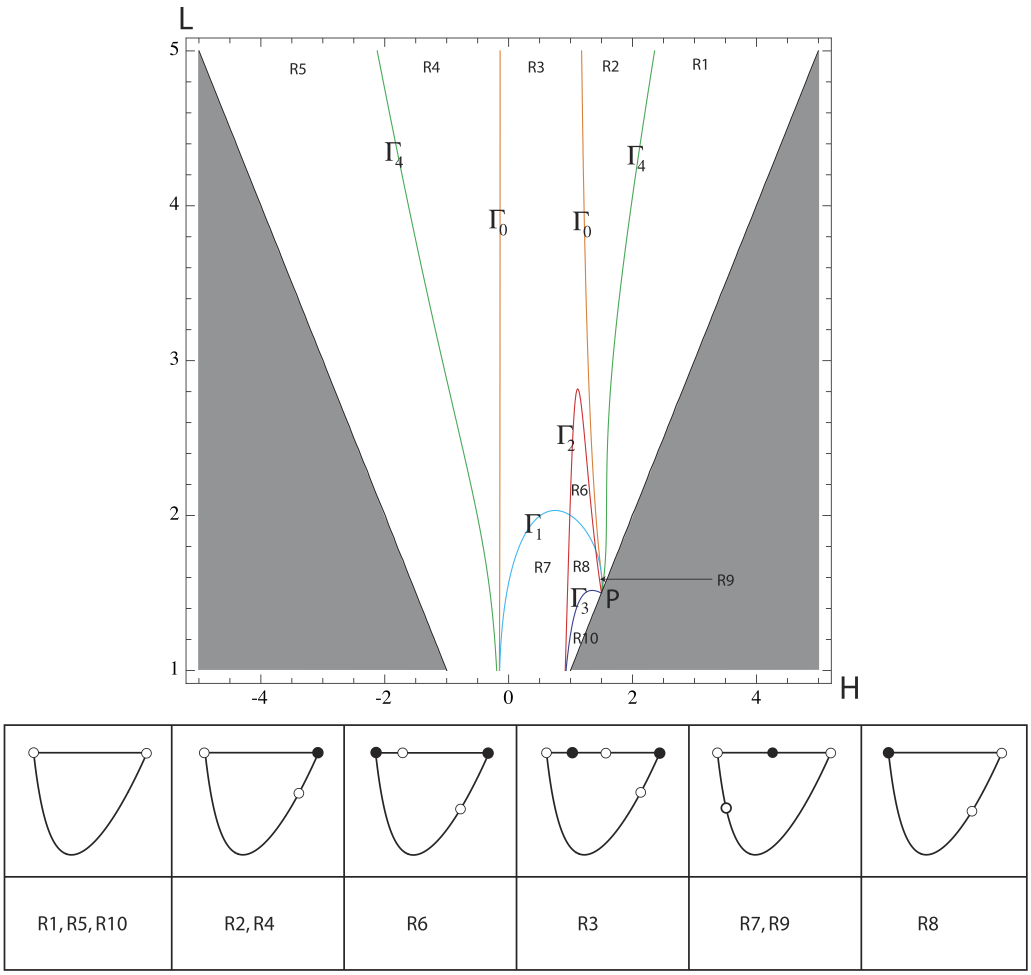

Fig. 8. The bifurcation plane (H, L) for $\delta = -0.02$, $\beta = 0.40649$ and $J_2 = 0.016298$ with the ten different regions it is divided into. Below, the critical points for each region: a black dot means instability (saddle), a white dot means stability (centre).

of δ the curve giving rise to a saddle-connection bifurcation does not enter the regions $R12$ and $R16$ when using the values of the parameters given in Fig. 5, and it is in contrast to what occurred for $J_2 = 0$. However, for negative values of δ, the curve arising from making the energies of circular and equatorial motions identical, which is given by

$$\gamma = -2\,\delta\,L^2\,H\,(\beta\,L^3\,H^2 + \beta\,L^2\,H^3 - 2\,L^2 - 2\,L\,H - 2\,H^2) + J_2\,(2\,L^4 + 2\,L^3\,H + 2\,L^2\,H^2 + 3\,L\,H^3 + 3\,H^4),$$

enters the region $R6$ for the values of δ, β and J_2 given in Fig. 8. It means that a saddle-connection bifurcation occurs between circular and equatorial relative equilibria and the stable/unstable branch of one of the saddle coincides with the unstable/stable branch of the other saddle.

It is also possible that saddle-connection bifurcations involving circular and equatorial solutions appear for other values of the parameters. Furthermore it is possible that saddle connections between circular and non-circular equilibria could occur (in the regions $R9$, $R15$ for $\delta > 0$ and in the region $R3$ for $\delta < 0$), but we have not checked it.

5.3. Stability of the relative equilibria in one degree of freedom

We consider the reduced Hamiltonian (12) and deal with the stability character of their equilibria, that is, the linear and nonlinear stability of the relative equilibrium points in a system of one degree of freedom. This is achieved by using the expression of the Hamiltonian in Delaunay coordinates, given in (5). After neglecting the terms factorised by δ^2, we use the following scheme for each type of equilibrium, namely:

(i) We choose an adequate set of symplectic coordinates q, p in term of Delaunay elements in such a way that the equilibrium expressed in these coordinates corresponds to the origin. We put the normalised Hamiltonian (5) as a function of q and p.

(ii) In order to determine the linear stability of the equilibrium we expand the Hamiltonian (5) in a Taylor series around the origin up to degree two, obtaining in all the cases an expression of the form $c_{2,1}\,q^2 + c_{2,2}\,p^2$ after dropping constant terms.

(iii) A certain relative equilibrium whose quadratic part of its normal form is of the form $c_{2,1}\,q^2 + c_{2,2}\,p^2$ is linearly unstable, specifically a saddle, when $c_{2,1}\,c_{2,2} < 0$, whereas it is linearly stable, specifically a centre when $c_{2,1}\,c_{2,2} > 0$.

(iv) When adding higher-order terms, the nonlinear stability character of an equilibrium with normal form starting at $c_{2,1}\,q^2 + c_{2,2}\,p^2$ remains the same as the linear stability provided that $c_{2,1}\,c_{2,2} \neq 0$. The reason is that the reduced Hamiltonian represents an analytic function and $c_{2,1}\,q^2 + c_{2,2}\,p^2$ is a Morse function [34]. Thus, linear saddles become nonlinear saddles while linear centres become nonlinear centres.

(v) A bifurcation occurs when $c_{2,1} = 0$ or $c_{2,2} = 0$ and the corresponding equilibrium becomes degenerate as at least one of the eigenvalues of its linearisation is zero.

In Refs. [35,36] we have performed a similar analysis in the context of perturbed Keplerian systems. In both papers we have defined similar variables to the ones we use here, so the reader can consult detailed computations there.

The case when one of the coefficients $c_{2,1}$ or $c_{2,2}$ vanishes has been excluded from our stability analysis. Note that the two coefficients cannot vanish at the same time as only pitchfork and saddle-centre bifurcations occur in the problem. In these degenerate situations one should perform the corresponding analysis, taking into account the 4-jets, i.e., including terms of degree four in q and p. We do not perform this analysis in the paper, as a similar study has been done for the pitchfork bifurcation in [36]. We present the results for δ positive, as the case $\delta < 0$ is treated in the same way, the only difference being that the regions Rj change.

Now we have to consider different cases in accordance with the types of trajectories that are studied. In particular, the case of circular equatorial solutions cannot be analysed in the spaces $\mathcal{T}_{L,H}$ or $\mathcal{U}_{L,H}$, as these spaces get reduced to points for this type of motion. Indeed these solutions need to be studied in the first-reduced space, that is, on $S^2_L \times S^2_L$, and we have done it in the companion paper [27]. Thus, we deal with three possible situations:

(a) near-circular solutions;
(b) near-equatorial solutions;
(c) non-near-circular non-near-equatorial solutions.

We stress that in case (a) the solutions are not near-equatorial whereas in case (b) they are not near-circular.

(a) *Equilibria associated with the near-circular solutions.*

Circular-type solutions correspond with the point $(0, 0, L^2 - H^2)$ in the reduced phase space $\mathcal{T}_{L,H}$ and with E_2 on the fully-reduced phase space $\mathcal{U}_{L,H}$. As circular orbits cannot be defined with Delaunay variables, we use a combination of them, say,

$$q = \sqrt{2\,(L-G)}\,\cos g, \qquad p = \sqrt{2\,(L-G)}\,\sin g.$$

Expressed in these variables, circular motions have coordinates $(0, 0)$, as in this case $G = L$. We put the Hamiltonian (5) in these coordinates and perform a Taylor expansion up to degree two around the origin. The result after dropping constant terms is the function $c_{2,1}\,q^2 + c_{2,2}\,p^2$, where

$$\begin{aligned} c_{2,1} &= \frac{1}{8\,L^9}\Big(\delta\,L^2\,(3\,\beta\,L^2\,H^2 + \beta\,L^4 - 12\,H) \\ &\quad + 3\,J_2\,(L^2 - 5\,H^2)\Big), \\ c_{2,2} &= \frac{1}{8\,L^9}\Big(\delta\,L^2\,(5\,\beta\,L^2\,H^2 - \beta\,L^4 - 12\,H) \\ &\quad + 3\,J_2\,(L^2 - 5\,H^2)\Big). \end{aligned} \tag{18}$$

The sign of the coefficients of the quadratic terms determines the linear stability of the relative equilibrium, i.e. of the circular-type motions. The coefficient of q^2 vanishes precisely on the curve Γ_1, whereas the coefficient of p^2 is zero on the curve Γ_4. So, circular solutions change stability when crossing these curves in the parameter plane. In Fig. 5 a scheme of the fully-reduced phase space is represented in all the regions of the parameter plane. Each dot represents an equilibrium on $\mathcal{U}_{L,H}$.

When neither $c_{2,1}$ nor $c_{2,2}$ vanish $c_{2,1}\,q^2 + c_{2,2}\,p^2$ is a Morse function, thus the stability character of the circular motions remains when incorporating higher-order terms. In other words, we get nonlinear centres in the regions $R2$, $R3$, $R4$, $R6$, $R7$, $R10$, $R11$ and $R14$ and nonlinear saddles in the remaining regions.

(b) *Equilibria associated with the near-equatorial solutions.*

Equatorial motions correspond to the point $(0, 0, H^2 - L^2)$ in the reduced phase space $\mathcal{T}_{L,H}$ and with the point E_1 in the fully-reduced phase space $\mathcal{U}_{L,H}$. Delaunay variables are not properly defined for equatorial motions, so we use another adequate combination of them in order to analyse the stability of these solutions. In particular we take the symplectic coordinates

$$q = \sqrt{2\,(G - |H|)}\,\sin g, \qquad p = \sqrt{2\,(G - |H|)}\,\cos g.$$

Expressed in these coordinates, equatorial motions have coordinates $(0, 0)$. We apply the change of variables to the Hamiltonian (5) and perform a Taylor expansion up to degree two in q and p around the origin. After dropping constant terms we get $c_{2,1}\,q^2 + c_{2,2}\,p^2$, where

$$\begin{aligned} c_{2,1} &= \frac{3\,(\delta\,H + J_2)}{2\,L^3\,H^4} - \frac{\beta\,\delta}{L\,|H|\,(L + |H|)}, \\ c_{2,2} &= \frac{3\,(\delta\,H + J_2)}{2\,L^3\,H^4} - \frac{\beta\,\delta}{L^2\,(L + |H|)}. \end{aligned} \tag{19}$$

The sign of the coefficients of the quadratic terms determines the linear stability of the equilibrium. The coefficient of q^2 vanishes precisely on the curve Γ_3, whereas the coefficient of p^2 is zero on the curve Γ_2. So, equatorial solutions change their stability when crossing these curves in the parameter plane, see Fig. 5. The equilibrium is elliptic (a linear centre) if $c_{2,1}\,c_{2,2} > 0$ and a saddle if $c_{2,1}\,c_{2,2} < 0$.

When adding the terms of degree three and higher in q and p we deal with the nonlinear stability of the equatorial motions. Provided that $c_{2,1}\,c_{2,2} \neq 0$ the stability behaviour is the same as the linear one. That is, the linear centres become nonlinear centres, this occurs in regions $R1$, $R2$, $R4$, $R5$, $R6$, $R7$, $R8$, $R9$, $R10$, $R13$, $R14$ and $R15$, whereas the linear saddles are nonlinear saddles in the remainder of the plane of parameters.

(c) *Equilibria associated with the non-near-circular non-near-equatorial solutions.*

For this kind of solutions Delaunay coordinates are well defined and we can use them to carry out the computations. Thus, we introduce q and p by means of

$$q = g - g_0, \qquad p = G - G_0,$$

where (g_0, G_0) corresponds to the value of (g, G) at the equilibrium. In accord with the discussion of the relative equilibria of non-circular non-equatorial type made previously, we have two possibilities: (i) either $g_0 = 0$ and G_0 satisfies the degree six equation

$$\begin{aligned} &-4\,\beta\,\delta\,L^2\,G_0^6 - 8\,\beta\,\delta\,L\,H^2\,G_0^5 \\ &\quad - \Big(4\,\delta\,H\,(\beta\,L^2\,H - 3) - 3\,J_2\Big)\,G_0^4 + 6\,L\,(4\,\delta\,H - J_2)\,G_0^3 \\ &\quad + 3\,\Big(4\,\delta\,L^2\,H - J_2\,(L^2 - 5\,H^2)\Big)\,G_0^2 \\ &\quad + 30\,J_2\,L\,H^2\,G_0 + 15\,J_2\,L^2\,H^2 = 0 \end{aligned} \tag{20}$$

or (ii) $g_0 = \pi/2$ whereas G_0 satisfies

$$\begin{aligned} &4\,\beta\,\delta\,L^2\,G_0^6 - 3\,\Big(4\,\delta\,H\,(\beta\,L^2\,H - 1) + J_2\Big)\,G_0^4 \\ &\quad - 2\,L\,\Big(4\,\delta\,H\,(\beta\,L^2\,H - 3) + 3\,J_2\Big)\,G_0^3 \\ &\quad + 3\,\Big(4\,\delta\,L^2\,H - J_2\,(L^2 - 5\,H^2)\Big)\,G_0^2 \\ &\quad + 30\,J_2\,L\,H^2\,G_0 + 15\,J_2\,L^2\,H^2 = 0. \end{aligned} \tag{21}$$

In case (i), we have an equilibrium on the rectilinear part of the boundary of $\mathcal{U}_{L,H}$ given by $\sigma_1 = (L - |H|)^2$ under the restriction $|H| < \sigma_1 < L$, while σ_2 is one of the valid roots of the polynomial $\mathcal{P}$, indeed, the polynomial $\mathcal{P}$ is the same as the polynomial given in (20). In case (ii), we have an equilibrium on the curved part of the boundary of $\mathcal{U}_{L,H}$ given by $\sigma_1\,\sigma_2^2 = (\sigma_2^2 - L\,|H|)^2$ and $|H| < \sigma_2 < L$, where σ_2 corresponds to one of the valid roots of $\mathcal{Q}$, in other words, a root of the polynomial given in (21).

We apply the change of coordinates to the Hamiltonian (5), perform a Taylor expansion up to degree two in q and p around the origin, drop constant terms and get $c_{2,1}\, q^2 + c_{2,2}\, p^2$. In particular, in case (i) $c_{2,1}$ and $c_{2,2}$ are

$$\begin{aligned} c_{2,1} &= -\frac{\beta\,\delta\,(L-G_0)\,(G_0^2-H^2)}{L^2\,G_0^2\,(L+G_0)},\\ c_{2,2} &= 4\,\beta\,\delta\,L^2\,G_0^7 + 12\,\beta\,\delta\,L\,H^2\,G_0^6\\ &\quad + 6\left(2\,\delta\,H\,(\beta\,L^2\,H-2)+J_2\right)G_0^5\\ &\quad + 2\,L\left(2\,\delta\,H\,(\beta\,L^2\,H-18)+9\,J_2\right)G_0^4\\ &\quad - 9\left(8\,\delta\,L^2\,H - J_2\,(2\,L^2-5\,H^2)\right)G_0^3\\ &\quad - 3\,L\left(8\,\delta\,L^2\,H - J_2\,(2\,L^2-45\,H^2)\right)G_0^2\\ &\quad - 135\,J_2\,L^2\,H^2\,G_0 - 45\,J_2\,L^3\,H^2, \end{aligned} \tag{22}$$

while in case (ii) we get

$$\begin{aligned} c_{2,1} &= \frac{\beta\,\delta\,(L-G_0)\,(G_0^2-H^2)}{L^2\,G_0^2\,(L+G_0)},\\ c_{2,2} &= -4\,\beta\,\delta\,L^2\,G_0^7 + 6\left(4\,\delta\,H\,(\beta\,L^2\,H-1)+J_2\right)G_0^5\\ &\quad + 2\,L\left(4\,\delta\,H\,(4\,\beta\,L^2\,H-9)+9\,J_2\right)G_0^4\\ &\quad + 3\left(4\,\delta\,L^2\,H\,(\beta\,L^2\,H-6)+3\,J_2\,(2\,L^2-5\,H^2)\right)G_0^3\\ &\quad - 3\,L\left(8\,\delta\,L^2\,H - J_2\,(2\,L^2-45\,H^2)\right)G_0^2\\ &\quad - 135\,J_2\,L^2\,H^2\,G_0 - 45\,J_2\,L^3\,H^2. \end{aligned} \tag{23}$$

In case (i) the coefficients $c_{2,1}$ and $c_{2,2}$ do not vanish for the equilibria on the rectilinear part of the boundary of $\mathcal{U}_{L,H}$, thus their stability character is the same wherever they exist in the parameter plane (H, L) and for any value of δ. More specifically, they are always linear centres. We notice that G_0 has to be chosen as a valid root of the polynomial (20).

For the equilibria on the curved part of the boundary of $\mathcal{U}_{L,H}$ (case (ii)), the coefficient $c_{2,1}$ does not vanish, whereas $c_{2,2}$ vanishes just at the curve Γ_5. So, the stability of these equilibria changes when the curve Γ_5 is crossed in the parameter plane (H, L). Here G_0 is an allowed root of (21). We have verified that $c_{2,1}\, c_{2,2} > 0$ for the centres and $c_{2,1}\, c_{2,2} < 0$ for the saddles. Furthermore, $c_{2,2} = 0$ when the parameters are taken on the curve Γ_5.

Finally, the linear centres remain nonlinear centres and the linear saddles remain nonlinear saddles when adding the nonlinear terms, since $c_{2,1}\, q^2 + c_{2,2}\, p^2$ is a Morse function provided that $c_{2,1}\, c_{2,2} \neq 0$ for all combinations of the parameters. Hence, the linear centres of regions $R1, R3, R4, R5, R8, R9, R10, R11, R12, R13, R15, R16$ are also nonlinear centres while the linear saddles of regions $R4, R9, R10, R15$ are nonlinear saddles.

6. Reconstruction of the flow

We analyse the existence of invariant 2-tori related with the relative equilibria of the fully-reduced Hamiltonian and of KAM 3-tori surrounding the 2-tori when they correspond with centres. We also reconstruct the occurring bifurcations of the 2-tori from the different bifurcations that take place in the fully-reduced phase space.

6.1. Invariant 2-tori and their bifurcations

After normalising the Hamiltonian $\mathcal{H}$ we have truncated the higher-order terms only once. This has allowed us to compute the first-reduced Hamiltonian on the first-reduced phase space $S_L^2 \times S_L^2$. The second reduction has been performed due to the fact that H is an integral related to a continuous symmetry (the axial symmetry) of the Hamiltonian $\mathcal{H}$ that is inherited by the averaged and reduced Hamiltonians. However, in contrast to L, the action H is an exact integral and no averaging and truncation have been needed to perform the second reduction. Thus, we can apply the techniques of [37] and those appearing in [38], and associate one or two invariant 2-tori (indeed families of 2-tori) to each non-degenerate relative equilibrium, i.e. to each equilibrium for which $c_{2,1}\, c_{2,2} \neq 0$, and these tori do exist as solutions of the Hamiltonian system defined by (1).

We make the reconstruction in stages, starting from the fully-reduced space.

(i) As the reduction from $\mathcal{T}_{L,H}$ to $\mathcal{U}_{L,H}$ is exact, each relative equilibrium on $\mathcal{U}_{L,H}$ (with $|H| \geq 0$) is straightforwardly associated with one, two or four families of invariant 2-tori in the original Hamiltonian. In our particular case, the points E_1 and E_2 reconstruct to one single family of invariant 2-tori, either of equatorial type (E_1) or of circular type (E_2). The remaining relative equilibria reconstruct to two families of invariant 2-tori because they are on the boundary of $\mathcal{U}_{L,H}$ and the points on this boundary (excepting E_1 and E_2) are related to two points on the space $\mathcal{T}_{L,H}$ due to the discrete symmetries $\mathcal{R}_1$ and $\mathcal{R}_2$).

(ii) The reconstruction from $\mathcal{T}_{L,H}$ to $S_L^2 \times S_L^2$ is also immediate, as the inverse reduction process is exact. Also, as the problematic points of $\mathcal{T}_{L,0}$ (i.e. the two corners of the sphere) are excluded from our study since the original problem is singular for $G = 0$, each equilibrium of $\mathcal{T}_{L,H}$ is related to a family of periodic solutions in $S_L^2 \times S_L^2$ depending on H. The stability (linear and orbital) of these periodic solutions is the same as the stability of the relative equilibria in $\mathcal{T}_{L,H}$ and in $\mathcal{U}_{L,H}$. The bifurcations of the relative equilibria are translated into the bifurcations of the same type of the periodic solutions in $S_L^2 \times S_L^2$.

(iii) The passage from $S_L^2 \times S_L^2$ to $\mathbb{R}^6$ relies on the reconstruction theory related to averaging theory, see [19,37], as the process involved the truncation of the higher-order terms. Equilibria of $S_L^2 \times S_L^2$ would correspond to families of periodic solutions in $\mathbb{R}^6$ and periodic solutions of $S_L^2 \times S_L^2$ are related to families of 2-tori in $\mathbb{R}^6$. The theorem ensuring this assertion is a *mutatis mutandis* translation (a slight generalisation) of Reeb's theorem and can be proved using the Hamiltonian flow box theorem (Lemma 2.1 of [38]), where in the set of coordinates $y = (y_2, \ldots, y_n, y_{n+2}, \ldots, y_{2n})$ there are two coordinates, say (y_2, y_{n+2}), which are a pair of action-angle variables and do not play any essential role in the Hamiltonian (formula (1) of [38, p. 315]). For the case considered in this paper this pair is (H, h) whereas the essential action-angles are (L, ℓ). Thus, to each point of the periodic solution one attaches a circle parametrised by h and H, obtaining a 2-torus. Moreover, the stability of the relative equilibria in $\mathcal{U}_{L,H}$ and $\mathcal{T}_{L,H}$ is inherited by the corresponding periodic solutions in $S_L^2 \times S_L^2$ and this stability character is translated to the 2-tori in $\mathbb{R}^6$.

In all cases the tori depend on the values of L and H (with $0 \leq |H| < L$ and $L > 1$) and are parametrised by two angles. These angles are ℓ and h for motions that are not of circular or equatorial type, while other combinations of the angles ℓ, g and h have to be taken for the tori related to the points E_1 and E_2, see the details in [4]. When ℓ and h are chosen to parametrise a single torus, their frequencies are given by the partial derivatives of the normal form Hamiltonian with respect to L and H respectively. Thus, the frequency related to ℓ is given by L^{-3} plus smaller terms of order δ while the frequency of h starts with terms factorised by δ. Note that the main term in the frequency of ℓ is the mean motion of the pure Keplerian part, a known fact for perturbed Keplerian systems.

The 2-tori are in general filled in with quasiperiodic solutions. More specifically, the quasiperiodic motions of the family of tori related to E_1 are near-equatorial but with any eccentricity $0 < e < 1$, while the quasiperiodic motions related to E_2 are near-circular but with any inclination I in $(0, \pi)$. The quasiperiodic solutions related to the remaining 2-tori have eccentricities close to the values $(1-(\sigma_2^*/L)^2)^{1/2}$ or $(1-(\sigma_2^-/L)^2)^{1/2}$ and inclinations close to $\arccos(H/\sigma^*)$ or $\arccos(H/\sigma^-)$ for the permitted values σ^* and σ^-. The study of near-circular near-equatorial motions is excluded from this analysis as the fully-reduced space is in this case a single point and its reconstruction needs to be made in $S_L^2 \times S_L^2$. Indeed this study was performed in [27], where we established the existence of 2-tori near-circular near-equatorial quasiperiodic motions of the system with Hamiltonian function (1).

We could have proceeded in a different way to achieve the existence of invariant 2-tori together with their stability character. Indeed, following [39], first the axial symmetry of the system can be used to reduce from $\mathbb{R}^6$ to a four-dimensional space that we call $\mathcal{B}_H$, through a singular reduction process. The system in $\mathcal{B}_H$ is a two-degrees-of-freedom Hamiltonian whose invariants appear in [39], see also [23]. Then the Keplerian symmetry should be applied to reduce to a space of dimension 2, which coincides with $\mathcal{T}_{L,H}$ because of the commutativity of the symplectic reduction by stages. The reduced Hamiltonian in $\mathcal{T}_{L,H}$ is $\mathcal{M}$. Then, the reconstruction from $\mathcal{T}_{L,H}$ to $\mathcal{B}_H$ allows us to relate the relative equilibria of $\mathcal{T}_{L,H}$ to families of periodic solutions in $\mathcal{B}_H$ sharing the stability character according to the theory devised in [38]. Note that even when $\mathcal{T}_{L,H}$ is singular for $H = 0$ we exclude rectilinear motions, so the results on the existence of periodic solutions and their stability given in [38] apply here. Then the families of periodic solutions of $\mathcal{B}_H$ are converted into families of invariant tori in $\mathbb{R}^6$ with the same stability behaviour when reconstructing to the initial problem.

The (linear) stability of the invariant 2-tori is the same as the parametric stability of the relative equilibria carried out in the previous section. In the case of one-degree-of-freedom Hamiltonians parametric stability is equivalent to linear stability, see [38], Theorem 2.2 and Corollaries 2.2 and 2.3. Thus, when the relative equilibria are not degenerate, the corresponding invariant tori have the same stability character as their counterparts in the fully-reduced phase space. It means that the invariant 2-tori are elliptic if the related equilibrium point is a centre or hyperbolic if the equilibrium is a saddle.

In the case of degeneracy, either $c_{2,1}$ or $c_{2,2}$ is zero and the analysis becomes delicate. Indeed these degeneracies occur when the relative equilibria bifurcate, either through a pitchfork or a saddle-centre bifurcation. However, we can ensure that the occurrence of the different bifurcations of relative equilibria on the fully-reduced space translates to the same occurrence of bifurcations of invariant 2-tori in the six-dimensional space where $\mathcal{H}$ is defined. Also, the discussion of the bifurcations depends on the internal parameters L and H and the physical parameters δ, β and J_2, although the bifurcation lines Γ_i appear a bit distorted due to the truncation process. Properly speaking we should say that the bifurcations depend on H and on L^*, which is obtained as $L^* = L - \partial\,\mathcal{W}_1/\partial\,\ell$, that is, L^* is the backward (inverse) transformation of L (an integral of $\mathcal{K}$) once we have dropped the higher-order terms. We stress that L^* is an approximate integral of $\mathcal{H}$, up to first-order terms.

As occurs with the saddle-centre bifurcation of periodic solutions [39,40], the families of invariant 2-tori that depend on L and H become degenerate for specific values of L^* and H (corresponding to a point on a bifurcation curve of the bifurcation plane). This critical value divides the family into a subfamily of elliptic 2-tori and a subfamily of hyperbolic 2-tori, exactly as happens with the saddle-centre and pitchfork bifurcation of equilibria. The linear stability of the degenerate tori is the same as the degenerate relative equilibria that they come from, that is, they are parabolic (unstable) invariant 2-tori.

We gather the above paragraphs in the following theorem.

Theorem 6.1. *The Hamiltonian of the generalised Størmer problem given through (1) has families of invariant 2-tori filled in with quasi-periodic solutions that are either of near-circular, near-equatorial and non-near-circular non-near-equatorial character. Also, one of the frequencies of the tori is L^{-3} plus higher-order terms whereas the other one is always much smaller. The (linear) stability character of these 2-tori is the same as the stability of the relative equilibria they are related to. The bifurcation diagram that occurs for the fully-reduced Hamiltonian is mimicked by a bifurcation diagram of invariant 2-tori with the lines Γ_i slightly distorted, thus saddle-centre and pitchfork bifurcations among 2-tori take place for the Hamiltonian (1). The description of these bifurcations in terms of the appearance and disappearance of the tori, their stability and degeneracy is the same as the description of the saddle-centre and pitchfork bifurcations of equilibrium points.*

We add that although the terms of δ^2 have not been included in the analysis of the reduced Hamiltonian, it does not mean that the conclusions about the existence, stability and bifurcations of the 2-tori of Hamiltonian (1) are strongly altered.

Finally, the saddle connection between the relative equilibria E_1 and E_2 obtained in Section 5 leads to saddle connections between families of 2-tori with quasiperiodic solutions near circular trajectories with quasiperiodic solutions being equatorial. Then, the three-dimensional stable manifold of a single torus (after fixing L and H) gets connected to the three-dimensional unstable manifold of another single torus. However, this should be proved rigorously, but as it is not an easy task we have not pursued this issue further.

6.2. KAM 3-Tori associated with the relative equilibria

Related with the centres studied in the previous section we can deduce the existence of KAM 3-tori of the system defined through the Hamilton function $\mathcal{H}'$ (and $\mathcal{H}$), using a local analysis in the vicinity of each relative equilibria of elliptic character. Specifically, the KAM 3-tori that we are discussing surround the invariant 2-tori established in the last subsection.

Proceeding similarly to what we did in [27] for the near-circular near-equatorial trajectories, we need to introduce a fictitious small parameter of the size of the small parameter of the problem. We distinguish among the 3-tori related with near-circular, near-equatorial or non-near-circular non-near-equatorial motions.

In the three cases we define q and p in terms of the Delaunay coordinates in the same manner as we have done for the stability of the relative equilibria, pushing the computations terms of degree two in q and p. We introduce action-angle coordinates around each equilibrium, indeed we define

$$q = \sqrt{\delta}\,\sqrt{2\,\Phi/\omega}\,\sin\phi, \qquad p = \sqrt{\delta}\,\sqrt{2\,\Phi\,\omega}\,\cos\phi,$$

with ω chosen adequately so that $c_{2,1}\,q^2 + c_{2,2}\,p^2$ becomes a multiple of Φ. The transformation is symplectic with multiplier δ, thus we need to divide the averaged Hamiltonian, including the Kepler term, by δ. Also we make the scaling $J_2 \to \delta\,\tilde{J}_2$ in order to emphasize that J_2 is a small parameter of the same size as δ.

Immediately, we recover the initial scaling of the system by doing $\Phi \mapsto \delta^{-1}\Phi$, and multiplying the whole Hamiltonian by δ. The resulting Hamiltonian is of the form

$$\mathcal{K} = -\frac{1}{2L^2} + \delta\,\mathcal{K}_1^{(1)}(L, H, \Phi) + \mathcal{O}(\delta^2)$$

where $\mathcal{K}_1^{(1)}$ is the normal form of degree two in q and p that come from $\mathcal{K}_1$ after making all the changes described above. This Hamiltonian depends on the three actions L, H and Φ, but it does not depend on the three respective angles ℓ, h and ϕ, as these angles appear at higher orders, starting at terms of order δ^2. Focusing on $\mathcal{K}_1^{(1)}$, it is given by $2\,(\tilde{c}_{2,1}\,\tilde{c}_{2,2})^{1/2}\,\Phi + F(L, H)$ and $\tilde{c}_{2,1}, \tilde{c}_{2,2}$ are obtained respectively from $c_{2,1}, c_{2,2}$ defined in (18), (19), (22) or (23), after replacing J_2 by $\tilde{J}_2$ and setting $\delta = 1$.

The explicit expression of the Hamiltonian $F(L, H)$ is one of the following functions

$$F_c(L, H) = \frac{2\beta L^6 + 2\beta L^4 H^2 + (\tilde{J}_2 - 4H) - 3\tilde{J}_2 H}{4L^8},$$

$$F_e(L, H) = -\frac{(2H + \tilde{J}_2)(L + |H|)}{2L^3 H^2 (L|H| + H^2)} + \frac{\beta}{L^2},$$

$$F_{g=0}(L, H) = \frac{\beta L^2 G_0^3 + LH(\beta H G_0^2 - 1) - H G_0}{L^3 (L + G_0) G_0^3} + \frac{\tilde{J}_2 (G_0^2 - 3H^2)}{4L^3 G_0^5},$$

$$F_{g=\pi/2}(L, H) = \frac{\beta L G_0^4 - (\beta L^2 H - 1) H G_0}{L^3 (L + G_0) G_0^3} + \frac{\tilde{J}_2 (G_0^2 - 3H^2)}{4L^3 G_0^5},$$

where F_c refers to the case of circular motions, F_e to equatorial motions, and $F_{g=0}, F_{g=\pi/2}$ to non-circular and non-equatorial motions. Also, G_0 is a valid root of (20) in $F_{g=0}$ and a valid root of (21) in $F_{g=\pi/2}$.

The Hamiltonian

$$-\frac{1}{2L^2} + \delta\,\mathcal{K}_1^{(1)}(L, H, \Phi)$$

is usually called the intermediate Hamiltonian.

Now, since the unperturbed part of the Hamiltonian depends only on the action L and $\partial\mathcal{K}_0/\partial\ell = L^{-3} \neq 0$, the Hamiltonian $\mathcal{K}$ is properly degenerate. However, if the perturbation removes the degeneracy, then the Hamiltonian system has invariant tori. We obtain these invariant tori by applying a KAM theorem for properly-degenerate Hamiltonians (Theorem 6.17, p. 279 of [41]) for the three types of motion we have classified. Hence, if for a certain equilibrium of the fully-reduced space the determinant of the matrix

$$\begin{pmatrix} \dfrac{\partial^2 \mathcal{K}_1^{(1)}}{\partial H^2} & \dfrac{\partial^2 \mathcal{K}_1^{(1)}}{\partial H\,\partial\Phi} \\[2mm] \dfrac{\partial^2 \mathcal{K}_1^{(1)}}{\partial\Phi\,\partial H} & \dfrac{\partial^2 \mathcal{K}_1^{(1)}}{\partial\Phi^2} \end{pmatrix}$$

is not zero then the perturbation removes the degeneracy.

In the case of circular-type motions this determinant is given by the quotient $D_c = n_c^2/d_c$ with

$$\begin{aligned} n_c \;=\;& \beta^2 L^{10} H + 15\beta^2 L^8 H^3 - 12\beta L^6 H (6H - \tilde{J}_2) \\ &+ 6L^4 \left(12H - \tilde{J}_2 (20\beta H^3 + 3)\right) \\ &+ 45\tilde{J}_2 L^2 H (6H - \tilde{J}_2) + 225\tilde{J}_2^2 H^3, \\ d_c \;=\;& 4L^{18}\left(\beta L^4 (L^2 - 5H^2) + 3L^2 (4H - \tilde{J}_2) + 15\tilde{J}_2 H^2\right) \\ &\times \left(\beta L^4 (L^2 + 3H^2) - 3L^2 (4H - \tilde{J}_2) - 15\tilde{J}_2 H^2\right), \end{aligned}$$

which is generically a well defined function that does not vanish for the allowed values of the parameters, moreover it is bounded from below by a function that does not tend to zero when $\delta \to 0$. Thus, the perturbation removes the degeneracy and there are KAM 3-tori associated with solutions of circular type, in such a way that the 3-tori surround the invariant 2-tori containing the near-circular solutions.

For the case of equatorial motions we obtain the determinant as the quotient $D_e = n_e^2/(L^6 H^{10} (L + |H|)^4 d_e)$ where

$$\begin{aligned} n_e \;=\;& \beta L^4 H^2 |H| (2\beta H^4 - 12H - 15\tilde{J}_2) \\ &+ 3L^3 (2\beta^2 H^8 - 12\beta H^5 - 15\beta\tilde{J}_2 H^4 \\ &+ 9H^2 + 21\tilde{J}_2 H + 12\tilde{J}_2^2) - 9L^2 |H| (4\beta H^5 \\ &+ 5\beta\tilde{J}_2 H^4 - 9H^2 - 21\tilde{J}_2 H - 12\tilde{J}_2^2) \\ &- 3LH^2 (4\beta H^5 + 5\beta\tilde{J}_2 H^4 - 27H^2 - 63\tilde{J}_2 H \\ &- 36\tilde{J}_2^2) + 9H^2 |H| (H + \tilde{J}_2)(3H + 4\tilde{J}_2), \\ d_e \;=\;& -2\beta L^3 H^2 |H| (2\beta H^4 - 3H - 3\tilde{J}_2) \\ &+ 3L (L + 2|H|)(4\beta H^4 - 3H - 3\tilde{J}_2)(H + \tilde{J}_2) \\ &+ 9H^2 (H + \tilde{J}_2)^2. \end{aligned}$$

In general this determinant is not zero and it is bounded from below with a function that cannot be zero when $\delta \to 0$, which means that the KAM theorem for properly-degenerate systems applies and there are KAM 3-tori related to the near-equatorial motions, in particular surrounding the invariant 2-tori of equatorial type.

Similarly to the cases of circular and equatorial motions we have computed the determinant corresponding to the relative elliptic equilibria that are neither of circular nor of equatorial type and we call it D_{nce}. We do not give the determinant here as it is too large, but we have checked that it is bounded from below by a function that does not tend to zero as δ tends to zero. Thus we conclude that there are KAM 3-tori related to the non-near-circular non-near-equatorial solutions. More precisely, these 3-tori surround the invariant 2-tori containing the non-near-circular non-near-equatorial solutions.

We encapsulate the analysis made in the above paragraphs in the following theorem.

Theorem 6.2. *The Hamiltonian of the generalised Størmer problem given through (1) has invariant KAM 3-tori surrounding the invariant 2-tori filled in with near-circular, near-equatorial and non-near-circular non-near-equatorial solutions, which correspond to the relative equilibria in one degree of freedom that are centres. These KAM tori form a majority in the sense that the measure of the complement of their union is small together with the perturbation. Also, the KAM tori are close to the invariant tori of the intermediate system* $-1/(2L^2) + \delta\mathcal{K}_1^{(1)}$. *The phase curves wind around these tori conditionally periodically with three frequencies. One frequency corresponds to the fast phase* ℓ, *and the other two to the slow phases* h *and* ϕ. *In particular the frequencies related to* h *and* ϕ *are respectively given by* $\delta\,\partial\mathcal{K}_1^{(1)}/\partial H + \mathcal{O}(\delta^2)$ *and* $\delta\,\partial\mathcal{K}_1^{(1)}/\partial\Phi + \mathcal{O}(\delta^2)$.

The above theorem for properly-degenerate Hamiltonians cannot be applied for a specific class of motion if its corresponding determinant (either D_c, D_e or D_{nce}) vanishes or is not well defined. In terms of the small parameter δ, the excluding measure of the invariant tori is small when δ is small.

We stress that we have dropped the terms of δ^2 in the analysis of the reduced Hamiltonian, but the conclusions on the KAM tori should differ only slightly from the analysis of this subsection, as the terms that would be incorporated to the determinants would not make them change drastically.

7. Conclusions

The dynamics of a charged particle orbiting a rotating magnetic planet is studied through a realistic model that takes into account the magnetic and the electric field as well as the gravitational potential of the planet, where the J_2-term is also included. We have focused on the case where the main force acting over the particle is the pure Keplerian term, thus our Hamiltonian lies in the setting of perturbed Keplerian systems. We have studied the dynamical features of the system using averaging and reduction theories, combining global with local methods conveniently.

Our main conclusions are summarised as follows:

(i) The analysis performed has been possible through a severe simplification of the original Hamilton function to a system of one degree of freedom, making the subsequent analysis valid for all eccentricities in the elliptic domain. Then we have applied reduction theory to give the averaged Hamiltonian its simplest possible form defined on the simplest reduced phase space. It has been achieved because we have taken into account all the continuous and discrete symmetries of Hamiltonian (1) and because we have averaged with respect to the mean anomaly at first order, truncating the higher-order terms.

(ii) This paper generalises [4] as we have included the perturbation caused by the oblateness of the planet. A complete analysis of the relative equilibria and their linear and nonlinear stability has been performed. The occurrence and type of stability of the equilibria depend on two internal parameters (the integrals of the averaged Hamiltonian, L and H) and three external parameters. Also, we have determined analytically the bifurcation lines, i.e. the relations satisfied by the parameters so that a change in the number of equilibria and stability occurs. The bifurcation diagram can have up to different sixteen regions.

(iii) We have established the existence of families of invariant 2-tori and quasiperiodic solutions for the Hamiltonian (1) reconstructed from the relative equilibria, sharing the same stability character (linearly). In particular, the particles get trapped in the stable 2-tori. Also, the bifurcation diagram on the fully-reduced phase space translates almost identically to a bifurcation diagram of invariant 2-tori of Hamiltonian (1) in terms of H and the inverse transformation of the action L, which is indeed an approximate integral of Hamiltonian (1).

(iv) We have proved the existence of invariant KAM 3-tori for the system (1) related to the elliptic relative equilibria of the fully-reduced Hamiltonian. It has been possible thanks to the application of a KAM theorem for properly-degenerate systems.

(v) Our work complements the study achieved in [27], where the analysis of the flow on the first-reduced phase space was made, focusing in particular on motions that are near-circular and near-equatorial. In that paper we reconstructed the families of periodic solutions together with their stability character related to the near-circular near-equatorial solutions and the KAM 3-tori surrounding the periodic solutions. The relative equilibria of the fully-reduced Hamiltonian in the present paper are transformed into families of periodic solutions on $S^2 \times S^2$ that depend on a fixed value of L but not on H. The linear stability of the families of periodic solutions is the same as the stability of the equilibria they come from. These families of periodic solutions bifurcate in the same manner as the relative equilibria they are related to and they are related to the families of invariant 2-tori in $\mathbb{R}^6$.

Acknowledgments

We appreciate the comments and suggestions made by the referees. Partial support to the authors has been received by Project MTM 2008-03818 of the Ministry of Science and Innovation of Spain.

References

[1] University of Colorado at Boulder, Press release: Cassini space-craft "sand-blasted" by dust from Saturn system in 2004, Saturday, January 22, 2005. http://www.spaceref.com/news/viewpr.html?pid=15968.
[2] C. Störmer, Sur les trajectories des corpuscules electrices, Arch. Sci. Phys. Nat. 24 (1907) 5–18. 113–158; 221–247.
[3] C. Störmer, The Polar Aurora, Clarendon Press, Oxford, 1955.
[4] M. Iñarrea, V. Lanchares, J. Palacián, A.I. Pascual, J.P. Salas, P. Yanguas, The Keplerian regime of charged particles in planetary magnetospheres, Physica D 197 (2004) 174–197.
[5] C. Grotta-Ragazzo, M. Kulesza, P.A.S. Salomão, Equatorial dynamics of charged particles in planetary magnetospheres, Physica D 225 (2007) 169–183.
[6] M. Horányi, Charged dust dynamics in the solar system, Annu. Rev. Astronom. Astrophys. 34 (1996) 383–418.
[7] J.E. Howard, M. Horányi, G.E. Stewart, Global dynamics of charged dust particles in planetary magnetospheres, Phys. Rev. Lett. 83 (1999) 3993–3996.
[8] J.E. Howard, H.R. Dullin, M. Horányi, Stability of halo orbits, Phys. Rev. Lett. 84 (2000) 3244–3247.
[9] H.R. Dullin, M. Horányi, J.E. Howard, Generalizations of the Størmer problem for dust grain orbits, Physica D 171 (2002) 178–195.
[10] M. Iñarrea, V. Lanchares, J. Palacián, A.I. Pascual, J.P. Salas, P. Yanguas, Reduction of some perturbed Keplerian problems, Chaos Solitons Fractals 27 (2006) 527–536.
[11] C.D. Murray, S.F. Dermott, Solar System Dynamics, Cambridge University Press, Cambridge, 1999.
[12] J.K. Campbell, J.D. Anderson, Gravity field of the saturnian system from Pioneer and Voyager tracking data, Astron. J. 97 (1989) 1485–1495.
[13] A.M. Fridman, N.N. Gor'kavyi, Physics of Planetary Rings: Celestial Mechanics of Continuous Media, Springer-Verlag, Berlin, New York, 1999.
[14] J.A. Burns, D.P. Hamilton, M.R. Showalter, Dusty rings and circumplanetary dust: observations and simple physics, in: E. Grun, B.A.S. Gustafson, S.F. Dermott, H. Fechting (Eds.), Interplanetary Dust, Springer, Berlin, 2001, pp. 641–725.
[15] A. Deprit, The elimination of the parallax in satellite theory, Celestial Mech. 24 (1981) 111–153.
[16] D. Brouwer, G.M. Clemence, Methods of Celestial Mechanics, Academic Press, New York, London, 1961.
[17] J. Henrard, Virtual singularities in the artificial satellite theory, Celestial Mech. 10 (1974) 437–449.
[18] A. Deprit, Canonical transformations depending on a small parameter, Celestial Mech. 1 (1969) 12–30.
[19] J. Moser, Regularization of Kepler's problem and the averaging method on a manifold, Comm. Pure Appl. Math. 23 (1970) 609–636.
[20] R.H. Cushman, Reduction, Brouwer's Hamiltonian, and the critical inclination, Celestial Mech. 31 (1983) 401–429. Correction: Celestial Mech. 33 (1984) 297.
[21] J.C. van der Meer, R.H. Cushman, Constrained normalization of Hamiltonian systems and perturbed Keplerian motion, Z. Angew. Math. Phys. 37 (1986) 402–424.
[22] R.H. Cushman, Normal form for Hamiltonian vectorfields with periodic flow, in: S. Sternberg (Ed.), Differential Geometric Methods in Mathematical Physics, D. Reidel Publishing Company, Dordrecht, 1984, pp. 125–144.
[23] J. Palacián, Normal forms for perturbed Keplerian systems, J. Differential Equations 180 (2002) 471–519.
[24] K.R. Meyer, C. Howison, Doubly-symmetric periodic solutions of the spatial restricted three-body problem, J. Differential Equations 163 (2000) 1386–1407.
[25] R.H. Cushman, D.A. Sadovskií, Monodromy in the hydrogen atom in crossed fields, Physica D 142 (2000) 166–196.
[26] S. Coffey, A. Deprit, B.R. Miller, The critical inclination in artificial satellite theory, Celestial Mech. 36 (1986) 365–406.
[27] M. Iñarrea, V. Lanchares, J. Palacián, A.I. Pascual, J.P. Salas, P. Yanguas, Symplectic coordinates on $S^2 \times S^2$ for perturbed Keplerian problems: application to the dynamics of a generalised Störmer problem, J. Differential Equations 250 (2011) 1386–1407.
[28] C.K. Goertz, G. Morfill, A model for the formation of spokes in Saturn's rings, Icarus 53 (1983) 219–229.
[29] J.E.P. Connerney, Magnetic connection for Saturn's rings and atmosphere, Geophys. Res. Lett. 13 (1986) 773–776.
[30] M. Tagger, R.N. Henriksen, R. Pellat, On the nature of spokes in Saturn's rings, Icarus 91 (1991) 297–314.
[31] G.E. Morfill, H.M. Thomas, Spoke formation under moving plasma clouds—the Goertz-Morfill model revisited, Icarus 179 (2005) 539–542.
[32] M. Iñarrea, V. Lanchares, J. Palacián, A.I. Pascual, J.P. Salas, P. Yanguas, The effect of J_2 on equatorial and halo orbits around a magnetic planet, Chaos Solitons Fractals 42 (2009) 155–169.
[33] V.V. Dikarev, Dynamics of particles in Saturn's E ring: effects of charge variations and the plasma drag force, Astronom. Astrophys. 346 (1999) 1011–1019.

[34] J. Milnor, Morse Theory, in: Ann. of Math. Stud., vol. 51, Princeton University Press, Princeton, NJ, 1963.
[35] J. Palacián, P. Yanguas, From the circular to the spatial elliptic restricted three-body problem, Celestial Mech. Dynam. Astronom. 95 (2006) 81–99.
[36] J. Palacián, Dynamics of a satellite orbiting a planet with an inhomogeneous gravitational field, Celestial Mech. Dynam. Astronom. 98 (2007) 219–249.
[37] G. Reeb, Sur certaines propriétés topologiques des trajectoires des systèmes dynamiques, Acad. Roy. Belgique. Cl. Sci. Mém. Coll. in 8° 27 (1952).
[38] P. Yanguas, J. Palacián, K.R. Meyer, H.S. Dumas, Periodic solutions in Hamiltonian systems, averaging, and the Lunar problem, SIAM J. Appl. Dyn. Syst. 7 (2008) 311–340.
[39] R.H. Cushman, S. Ferrer, H. Hanßmann, Singular reduction of axially symmetric perturbations of the isotropic harmonic oscillator, Nonlinearity 12 (1999) 389–410.
[40] M. El Samaloty, Averaging and bifurcation theory, Thesis, University of Cincinnati, 1984.
[41] V.I. Arnold (Ed.), Dynamical Systems III, in: Encyclopaedia of Mathematical Sciences, vol. 3, Springer-Verlag, New York, 1988.